AUTOMATIC COMPENSATION OF AN ELECTRO-ACOUSTIC SYSTEM

By

BUCK F. BROWN

Bachelor of Science

Massachusetts Institute of Technology

1955

Submitted to the faculty of the Graduate School of
the Oklahoma State University
in partial fulfillment of the requirements
for the degree of
MASTER OF SCIENCE
May, 1959

OKLAHOMA
STATE UNIVERSITY
LIBRARY

FEB 29 1960

AUTOMATIC COMPENSATION OF AN
ELECTRO-ACOUSTIC SYSTEM

Thesis Approved:

Paul A. McCollum
Thesis Adviser

Truet B. Thompson
Faculty Represenitive

Robert MacVicar
Dean of the Graduate School

438551

ACKNOWLEDGMENT

The author wishes to express his sincere thanks to Professor Paul A. McCollum for his guidance and support in this study. Appreciation is also extended to Mr. Glen T. Stotts for his assistance in the procurement of equipment and data.

PREFACE

During the past few years, the increased interest in high quality audio reproduction has led to the development of many fine electro-acoustic systems. The electronic portions of these systems have, for a considerable period of time, employed degenerative feedback. The merit of such an arrangement is beyond question. Application of the output of these fine amplifiers to present day electro-acoustic transducers has, however, produced much concern. These transducers introduce distortion and appear to be the weakest link in the reproduction chain.

This thesis is concerned with an extension of degenerative feedback to encompass both the speaker and power amplifier. The synthesis, design and experimental verification of two such closed loop systems is undertaken. Attention is focused on the response characteristics below 300 cycles per second, since reproducers, in general, have the poorest response in this region.

Overall performance is measured in terms of steady state frequency characteristics. This approach makes possible a graphical display of both the synthesis and the experimental response of each system. Conventional feedback asymptotic approximations are made with the result that lengthy mathematical expressions are held to a minimum.

TABLE OF CONTENTS

LIST OF PLATES

LIST OF TABLES

LIST OF FIGURES

LIST OF CURVES

CHAPTER I

INTRODUCTION

The growing demand for better electro-acoustical reproduction within the past decade has lead to several rather amazing results. The relatively high power levels (30 - 100 watts) involved in today's better sound systems and the wide concern with intermodulation and harmonic distortion were virtually nonexistent a few years ago. In addition to these items, the useful life of today's recordings has been lengthened by the development of materials and techniques now being employed by the industry.

One (1) of the major steps towards high quality reproduction was taken when Columbia introduced its Microgroove records. These vinylite pressings had several advantages over earlier discs. Longer playing time combined with an improved dynamic range, a wider frequency response, lighter allowable stylus pressures, longer record life and lessened background noise has lead to the wide acceptance of this form of recording. Doubtlessly the development of the low compliance magnetic or variable reluctance type of transducer has had much to do with the advancement of the art.

An early day sound reproduction system might be schematically represented by the diagram of Figure 1. Such a unit has serious limitations, however. The conventional audio amplifier introduces amplitude, phase and harmonic distortion for both low and high frequency

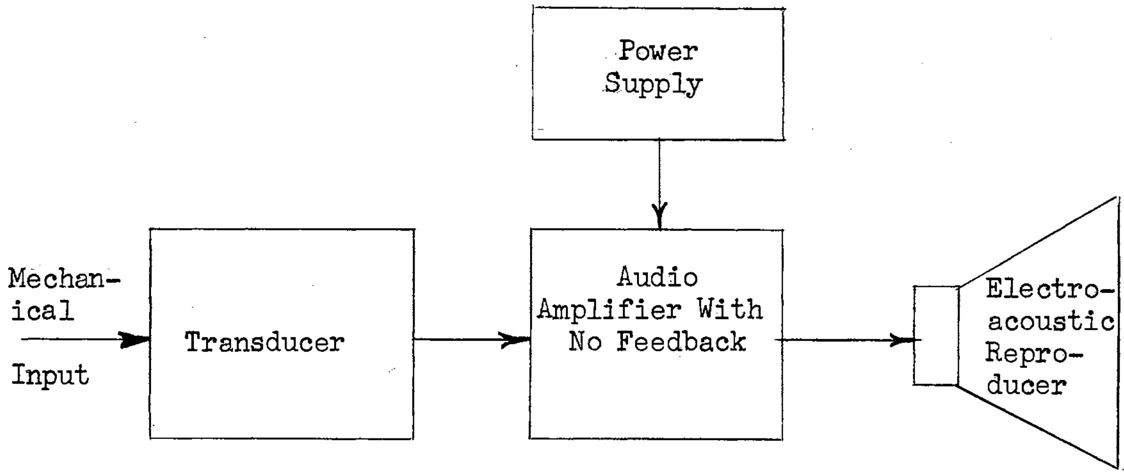

Figure 1.

An Early Sound System.

signals. Even if the sound reproducing unit performed perfectly*, the system would have a relatively low quality audio output.

The real need for superior amplifiers was recognized by audio engineers. A solution for this need developed as feedback principles became more fully understood. Multiple loop feedback amplifiers were developed having inaudible harmonic distortion and an extended frequency range. (2, 3).

In spite of these forward moving steps in electronics, the complete solution to the problem of faithful reproduction still remained hidden. Energy conversion, then and now, seemed to hold the key to the world of "high fidelity". This conversion must occur four times before the sound generated in the recording studio finally reaches the listener's ears.

---

*Here, the word, perfectly, implies a transfer function which is a constant. The result, of course, is a speaker characteristic independent of frequency.

There are few doubts as to the intentions of those connected with audio reproduction. These intentions have been clouded somewhat due to the popularization of audio terms by those who have little experience with and even less knowledge of the field. The expression "high fidelity", for instance, has become a household phrase; yet, little agreement seems to exist as to its real meaning. Most high fidelity reproduction is judged by the question, (1) "Does it sound pleasant or not?" Since pleasantness is one of the aesthetic quantities, this question affords little in the way of design criteria to the engineer. For that reason, the measure of performance will be taken as the faithfulness with which the system reproduces the input signal. The transfer function of an ideal system would be a constant; thus, introducing no unwanted frequency characteristics of its own. (4). The output sounds will be identical in harmonic content and phase to the input signal, regardless of its pleasantness or unpleasantness.

In order to achieve this goal of a constant transfer function, much work has been expended in the area of transducers. It would seem that the weakest link still remaining is the electro-acoustical reproducer or speaker. This device, when arranged in proper relation to other speakers by means of cross-over networks, approximates the desired transfer function from a few hundred cycles per second to beyond audibility. Below a few hundred cycles per second, the response varies widely from the ideal. In an effort to correct this non-ideal characteristic, various enclosures (5) have been designed to provide for the proper low frequency loading of the speaker. These enclosures must be well constructed, heavy cabinets with padding, tuned ports and correct dimensions.

Unfortunately, the results are far from perfect, while the cost often exceeds that of the remainder of the system. It would appear, as a matter-of-fact, that the upper limit of the present design technique has been reached in the development of quality audio systems. In order to proceed beyond this point some new approach must be recognized and employed.

Such a technique has been pointed out by several engineers interested in the audio field (6). The diagram of Figure 2 portrays a typical scheme. The interesting portion of the diagram is that depicted as velocity feedback around the speaker and transistorized servo amplifier. Such a system with certain feedback modifications would appear to be the most economical method of low frequency compensation possible. There are difficulties inherent in the technique, however. Of these, stability is probably the most outstanding, since low frequency drop-offs in the output appear with 12 to 18 db per octave slopes. This, of course, tends to increase the possibility of oscillation even with a degenerative feedback connection. In addition, it is apparent that such an arrangement is intended to control the velocity of the apex of the speaker cone. It will be demonstrated in later chapters that a one to one correspondence does not exist between the speaker cone apex velocity and the acoustical (pressure) output.

The text of this thesis is concerned with the synthesis and design of a more ideal sound reproducing unit. The verification of the design is undertaken experimentally in order to demonstrate the superiority of a closed loop system over one operating in a open loop fashion.

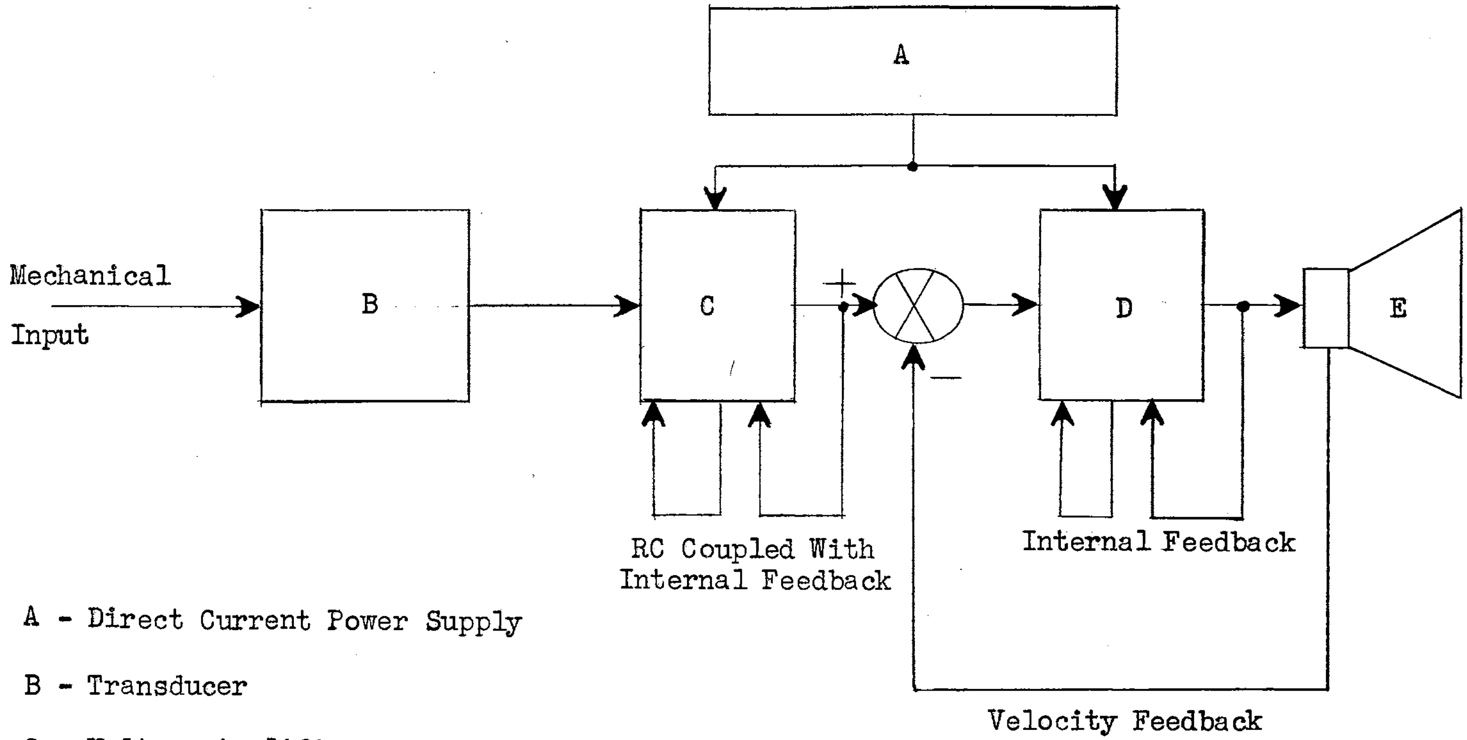

A - Direct Current Power Supply

B - Transducer

C - Voltage Amplifier

D - Transistorized Servo Amplifier

E - Electro-Acoustical Transducer

Figure 2.

An Automatically Controlled Speaker Employing Velocity Feedback.

CHAPTER II

THE LOUDSPEAKER

Physical Construction

Prior to embarking upon a design program it is appropriate to consider the action of a permanent magnet, diaphram type of electro-acoustic transducer. At present, almost all low frequency speakers fall into this classification. It is a well known fact (7) that speakers of this type have a characteristic coupling between the diaphram and the medium into which the sound is being radiated. In general, loss of this coupling at low frequencies is responsible for the 12 to 18 db per octave slope mentioned in Chapter I. Some of the most common methods employed to increase radiation in this range are namely, the use of large diaphragms, groups of diaphragms and various horns and baffles. In view of this and the scope of this thesis, a decision as to the size of the speaker was reached at a very early stage. The large baffle concept for higher performance in the low frequency range was chosen. In particular, a 12 inch diameter diaphram became the subject of the investigation.

In Figure 3, a detailed sketch of the construction of the speaker is shown (8, 9). It is noted that the system consists of a paper cone driven by a voice coil located in a magnetic field. It is desirable to write the equation of motion of the speaker relating the output (temporarily taken as the apex velocity) to the input. This input for

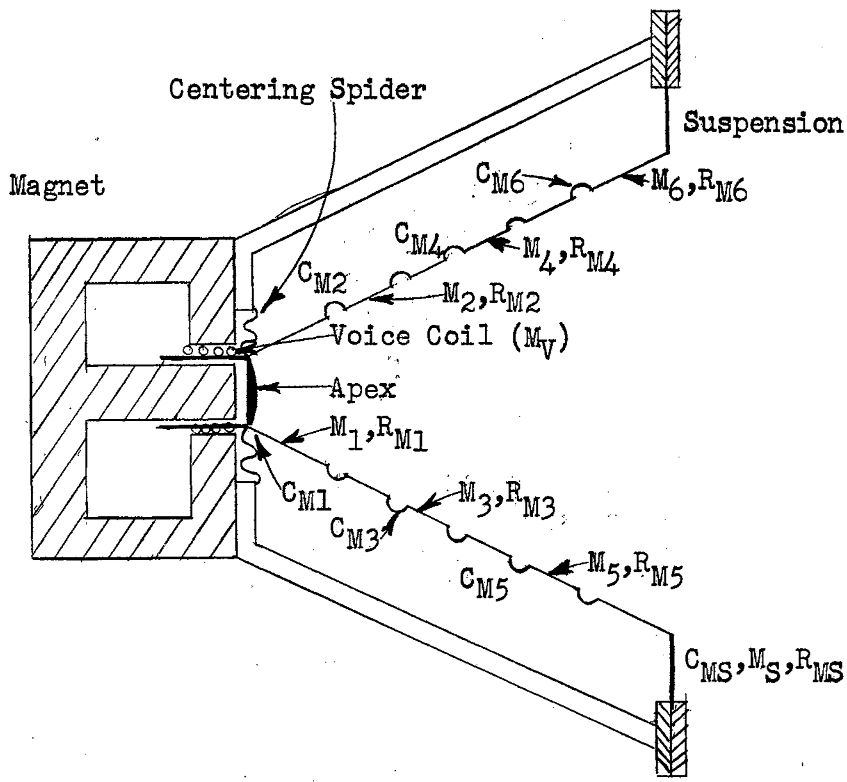

C_{MS} - Compliance of centering spider and suspension

M_V - Mass of voice coil

C_{M1} - Compliance of neck of cone

C_{M2}, C_{M3} • • • Compliance of the corrugations

M_1, M_2 • • • Mass of elements of the cone and air load

M_S - Mass of suspension

R_{MS} - Resistance of Suspension

R_{M1}, R_{M2} • • • Air load resistance

Figure 3.

Permanent Magnet Loudspeaker.

normal operation will be current to the voice coil. The force exerted by the interaction of the voice coil current and the magnetic field is given by the equation:

$$F = Bli \qquad (1)$$

where

B = the magnetic flux density,

l = the length of the conductor on the voice coil,

i = the instanteous value of current through the voice coil.

Equation of Motion

For extremely low frequencies, the entire cone will move as a unit. In so doing, a mass of air, M_A, will be moved as well as the mass of the cone, M_C, and voice coil, M_V. Opposing the displacement will be a force due to the product of the mass and acceleration. In addition, a frictional force will exist as well as a spring force. Expressed in mathematical form, this becomes

$$Bli = (M_A + M_C + M_V)\frac{d^2x}{dt^2} + R_{MA}\frac{dx}{dt} + \frac{x}{C_{MS}}, \qquad (2)$$

where x represents the displacement and R_{MA} is the sum of R_{M1}, R_{M2}, R_{M3}, R_{M4}, R_{M5}, and R_{MS}. For convenience of notation, let

$$(M_A + M_C + M_V) = M. \qquad (3)$$

The LaPlace Transform of equation (2) appears as equation (4) with B considered a constant. All initial conditions are zero.

$$BlI(S) = MS^2X(S) + R_{MA}SX(S) + \frac{X(S)}{C_{MS}} \qquad (4)$$

From this it can be seen that

$$\frac{X(S)}{I(S)} = \frac{Bl}{S(MS + R_{MA} + \frac{1}{C_{MS}S})} . \qquad (5)$$

Equation (5) represents the transfer function of the integral of the output over the input. To obtain the desired function, $\frac{\dot{X}(S)}{I(S)}$, it is necessary to multiply the existing transfer function, equation (5), by S. The result appears below:

$$\frac{\dot{X}(S)}{I(S)} = \frac{SX(S)}{I(S)} = \frac{BlS}{MS^2 + R_{MA} + \frac{1}{C_{MS}S}} \qquad (6)$$

or:

$$\frac{\dot{X}(S)}{I(S)} = \frac{Bl}{MS + R_{MA} + \frac{1}{C_{MS}S}} \qquad (7)$$

An Analogous Circuit

An analogy may be drawn at this point between equation (7) and that obtained from writing the Kirchhoff's voltage law equation for a series RLC circuit as shown in Figure 4. Such an equation

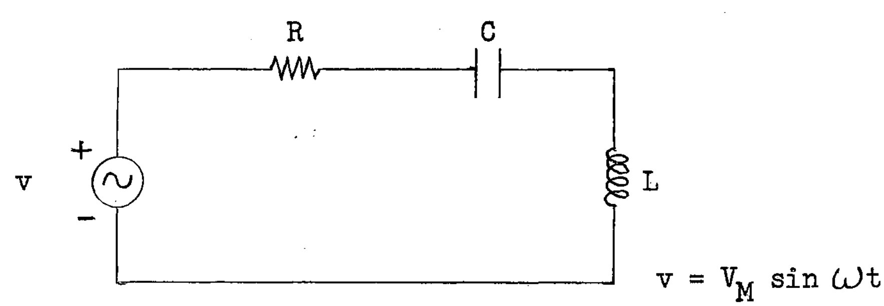

Figure 4. Equivalent Circuit of the Loudspeaker Mechanical System

written in terms of instantaneous values is:

$$v = Ri + L\frac{di}{dt} + \frac{1}{C}\int i\,dt \,. \tag{8}$$

The LaPlace Transformation of the equation with initial conditions again considered zero yields:

$$V(S) = I(S)R + LSI(S) + \frac{1}{C}I(S) \,. \tag{9}$$

Solving for the ratio of I(S) to V(S), the commonly encountered quantity, admittance or Y(S), is obtained.

$$Y(S) = \frac{I(S)}{V(S)} = \frac{1}{LS + R + \frac{1}{CS}} \,. \tag{10}$$

Inspection of equations (7) and (10) reveal certain similarities. The following Table indicates analogous quantities.

TABLE I

ANALOGOUS ELECTRICAL AND MECHANICAL QUANTITIES

Mechanical Equation (7)	Electrical Equation (10)
M	L
R_{MA}	R
C_{MS}	C
$\mathring{X}$	I
I	V

One item of difference between the equations appears as the constant multiplier, Bl, in equation (7). It will be seen, however, that the quality of total analogy is unaltered by the inclusion of this constant in the discussion.

One of the most popular methods of analysis relies upon the steady state frequency response characteristics of systems under consideration. Such a technique will be employed here. The results of such a method are usually displayed in the form of a Bode plot (10, 11). Under these conditions, the LaPlace operator "S" takes on the significance of $j\omega$ where ω is the radian frequency of the applied sinusoidal driving function. Much has been written concerning the analysis of the series RLC circuit (12, 13) for just such an input. The usual attempt is to establish a standard form for the transfer function and by the inspection of certain coefficients to determine the overall response as the frequency is varied. Equation (11) represents the standard form of a second order transfer function.

$$F(S) = \frac{AS}{\tau^2 S^2 + 2\tau\delta S + 1} \tag{11}$$

It is evident that proper factoring of equation (10) will produce a function of this nature.

$$Y(S) = \frac{CS}{LCS^2 + RCS + 1} \tag{12}$$

From comparison of equations (11) and (12) it is readily seen that:

$$\tau^2 = LC \tag{13}$$

$$\tau = \sqrt{LC} \tag{14}$$

and:

$$2\tau\zeta = RC = 2\sqrt{LC} \times \zeta \qquad (15)$$

or:

$$\zeta = \frac{RC}{2\sqrt{LC}} = \tfrac{1}{2} R\sqrt{C/L} \qquad (16)$$

while:

$$C = A \qquad (17)$$

If the denominator of Y(S) is factored, it is noted that the equation may have either real or complex roots. Solution for these roots leads to:

$$S = \frac{-2\tau\zeta \pm \sqrt{4(\tau\zeta)^2 - 4\tau^2}}{2\tau^2} \qquad (18)$$

or:

$$S = -\frac{\zeta}{\tau} \pm \frac{\sqrt{\zeta^2 - 1}}{\tau} \qquad (19)$$

The presence of the negative sign in front of the first term, $\frac{\zeta}{\tau}$, indicates system stability. Of equal importance, however, is the discriminate of equation (19). This quantity may have values in three very interesting ranges.

$$\zeta^2 - 1 > 0 \qquad (20)$$

$$\zeta^2 - 1 = 0 \qquad (21)$$

$$\zeta^2 - 1 < 0 \qquad (22)$$

Clearly, the value of ζ must be greater than unity if the first range is to exist. On the other hand $\zeta = 1$ will allow the discriminate to have a zero value, while for $\zeta < 1$ the discriminate will be negative. From this it can be seen that the condition of equation (20) produces real roots to the denominator and equation (22) leads to complex roots. Curve 1 is a plot of $\left[\tau^2 S^2 + 2\tau\zeta S + 1\right]^{-1}$. The shape of the curve, particularly around resonance, will deviate from that predicted by the Bode asymptote technique. The exact amount of deviation is a function of the value of ζ. For ζ approximately equal to one the error is only slight. Further analysis will be based upon the Bode asymptotes as illustrated by the dotted line on Curve 1.

Reference to equation (12) again, reveals that the numerator plot remains to be accomplished. Such a term, CS, appears as a straight line with positive slope on the frequency response plot. This is plotted in Curve 2.

One of the conveniences of making a transfer function plot in terms of decibels arises from the fact that curves may be graphically added when a numerical gain multiplication is desired. If for example, the asymptote from Curve 1 is added to Curve 2 the result is a curve representing the product of the two "S" functions. This is due, of course, to the fact that the decibel plot is proportional to the logarithm of the numerical plot. Putting it slightly different, the addition of the asymptote from Curve 1 to Curve 2 leads to the desired function, Y(S).

In the case at hand, CS is plotted against $\omega\tau$ in order to present a normalized frequency curve. The difference between the frequency scales of Curve 1 and Curve 2 should not go unnoticed. The value of τ is not the same in each case. It would be unreasonable to assume, then, that the product, $\omega\tau$, is in both cases identical.

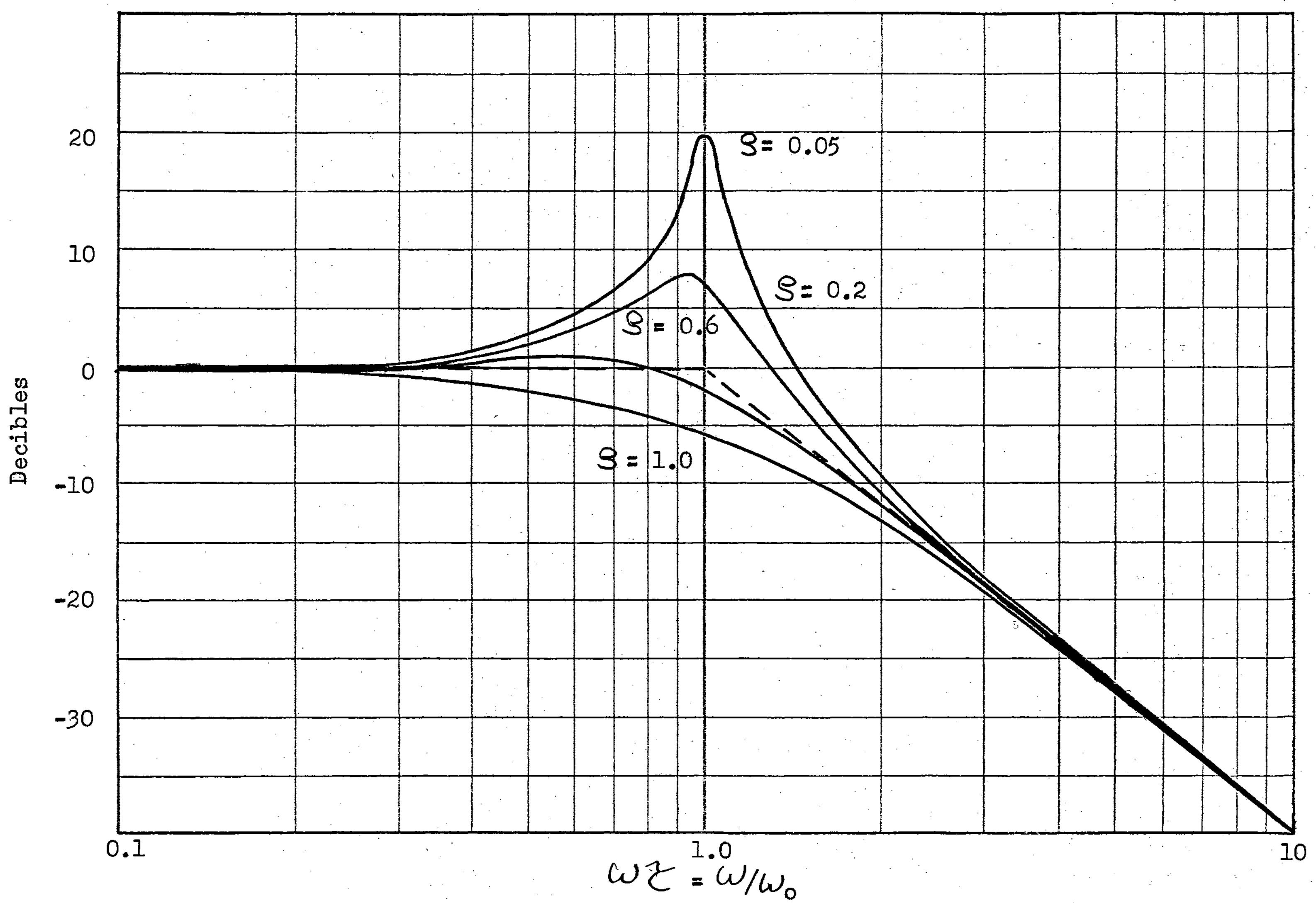

Curve 1. Plot of $\left[\tau^2 S^2 + 2\tau\zeta S + 1\right]^{-1}$ as a Function of $\omega\tau$.

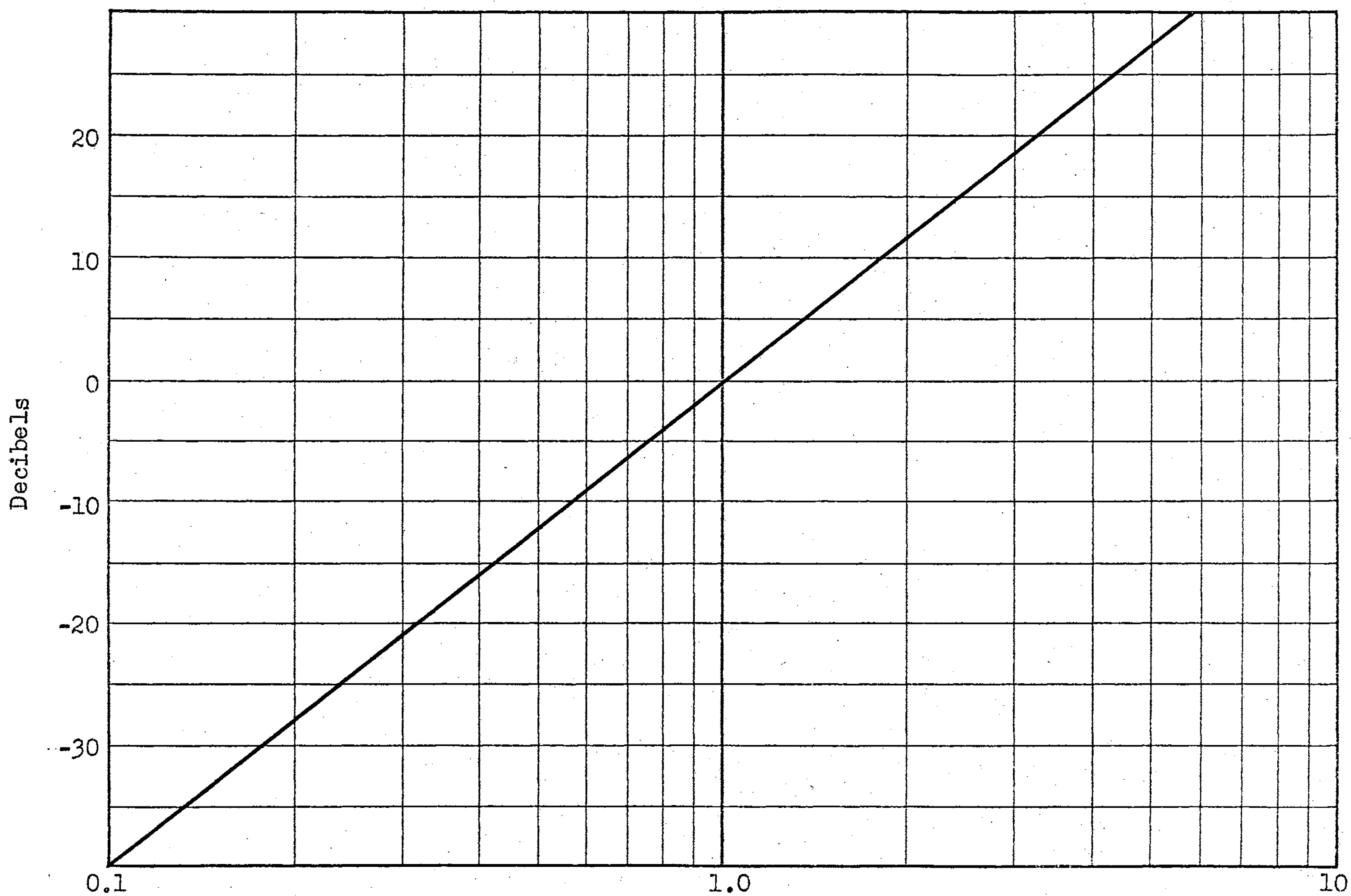

Curve 2. Plot of CS as a Function of $\omega\tau$.

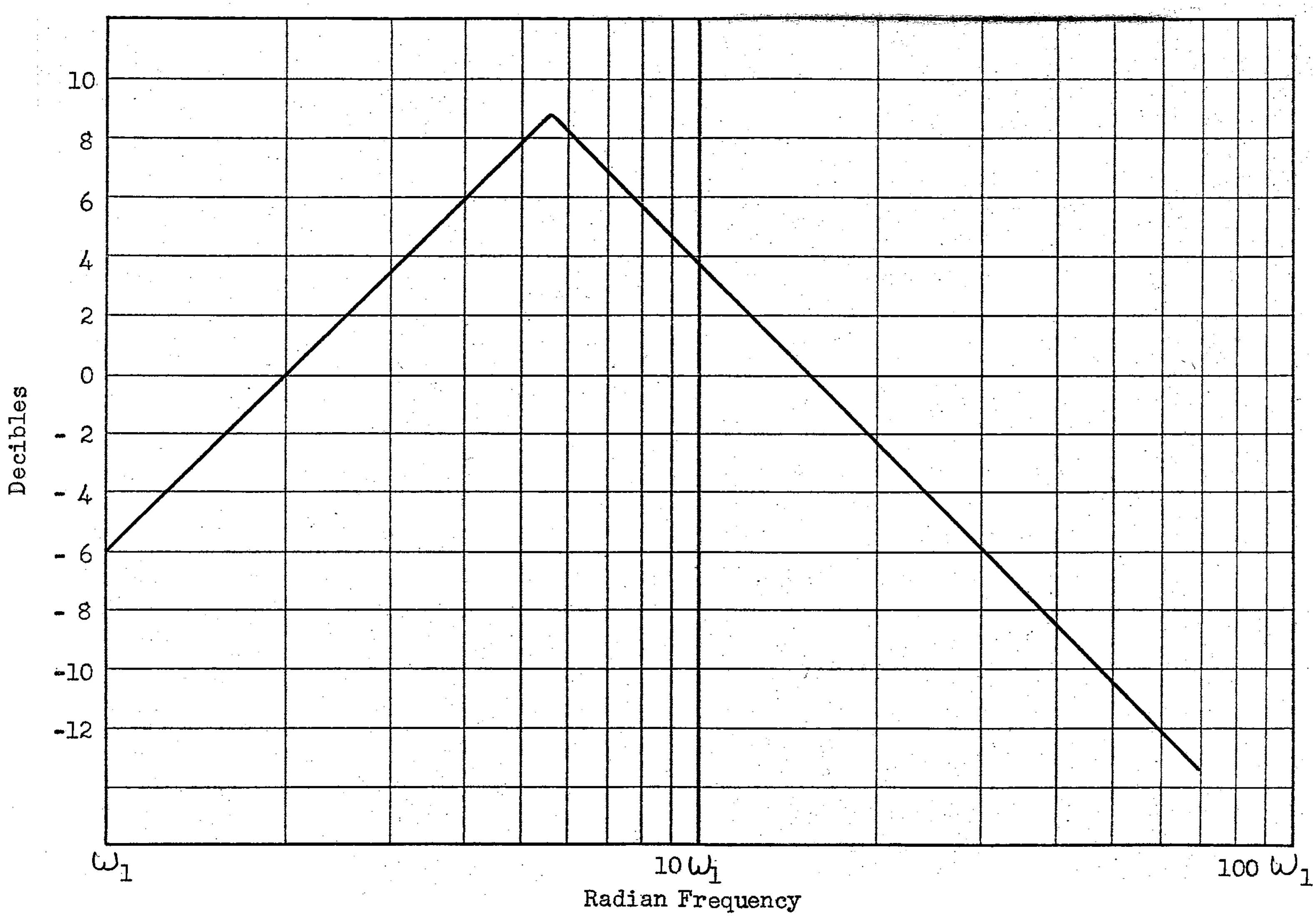

Curve 3. The Plot of Y(S) on a Non-Normalized Scale.

Therefore, a non-normalized plot of each function must be employed before the operation of addition can be performed. Since no numerical values are sufficiently general to fit the discussion, the resulting plot (Curve 3) is constructed with the horizontal frequency scale appearing as a function of a base frequency, ω_1.

The points of zero db axis crossing are of little importance as is the exact peak gain of the system. These may be altered by changing the values of the constants in the equation under consideration. It is interesting to note that the low frequency characteristics of the function, Y(S), are determined by the numerator of equation (12). The high frequency drop-off is at the rate of 6 db per octave as established by the denominator of the same equation. The question now comes to mind, "Does this curve have a positive db gain region or not?" The answer lies within the equation itself. If the constant multiplier of the numerator is sufficiently different in size from the square root (assuming the real root solution for the polynomial of the denominator) of the coefficient of S squared in the denominator then a positive db gain region may exist. One other provision is worthy of mention. The constant of the numerator will be larger than the square root of the coefficient of S squared in the denominator. This will prove to be an assumption of merit when a comparison of data is made with the predicted curve.

The Division of the Speaker Into Two Transfer Functions

Up to this point the discussion has dealt primarily with the equation for Y(S). Since a similarity has been established between

$Y(S)$ and the function $\mathring{X}/I$, the foregoing pertains equally well to this quantity. The constant multiplier, Bl, of equation (7), tends to accentuate the difference in the constant of the numerator and the square root of the coefficient of S squared in the denominator. The result is a curve exactly the same in shape as that of Curve 3. It will, in general, be displaced vertically from that shown. If the product, Bl, is larger than one then the curve will be shifted up. Conversely, a value of Bl less than one leads to a downward positioning of the plot.

In practice, the peak of Curve 3 usually appears in the range of 30 to 100 cycles per second. It is also true that the coupling effect between the diaphragm of the transducer and the mass of air, M_A, is active in this region. As a first approximation, it is assumed that the decoupling effect has begun at a higher frequency and attenuates at the rate of 6 db per octave. The resultant transfer function of the product of $\mathring{X}/I$ and the decoupling function appears as Curve 4. In order to gain more insight into the meaning of this product, reference is made to Figure 5. Here, the speaker is considered as a

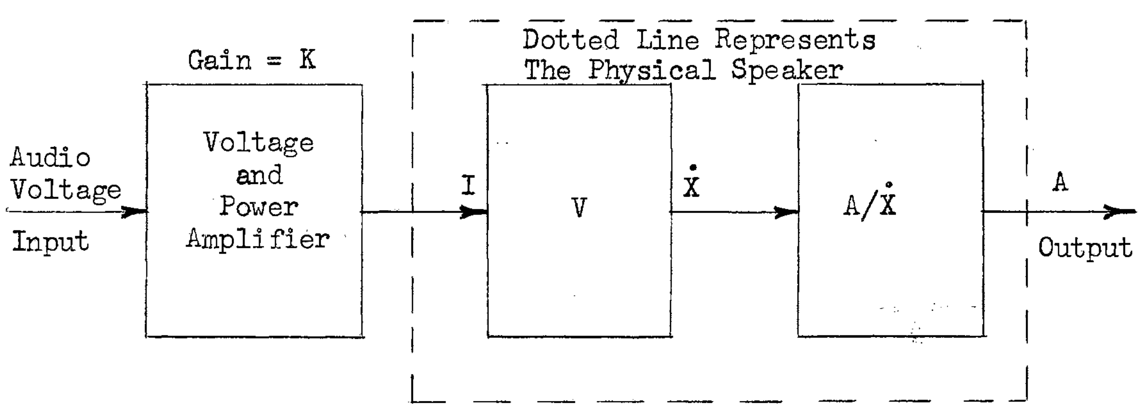

Figure 5. Block Diagram Illustrating the Division of a Speaker into Two Separate Transfer Functions.

two block unit. The first of these two blocks accounts for the input current, I, to the system and relates it directly through the gain function V (previously called $\dot{X}/I$) to the output velocity. In the future, this transfer function will be more completely entitled the velocity transfer function. The second of the two blocks indicates that a velocity input, $\dot{X}$, results in an acoustic output, A, through the function, $A/\dot{X}$. The total speaker gain is simply $V(A/\dot{X})$.

Unfortunately, it is not possible to simply predict the quantity $A/\dot{X}$. This function is most assuredly more complicated than the one presently under discussion. The purpose of this section has been to point out that a fast decrease in response must be expected as the frequency is lowered. This decrease may be attributed to both V and $A/\dot{X}$. It is also well to realize the possibilities for varied response around the velocity resonance region.

In passing, a comment concerning the block diagram of Figure 2 seems appropriate. This system has already been shown to be a velocity control feedback arrangement. Although such a scheme may tend to improve the response, it will not idealize the output by any means. Some manner of compensation must be supplied to the closed loop control of this speaker in order to provide for the decoupling effect.

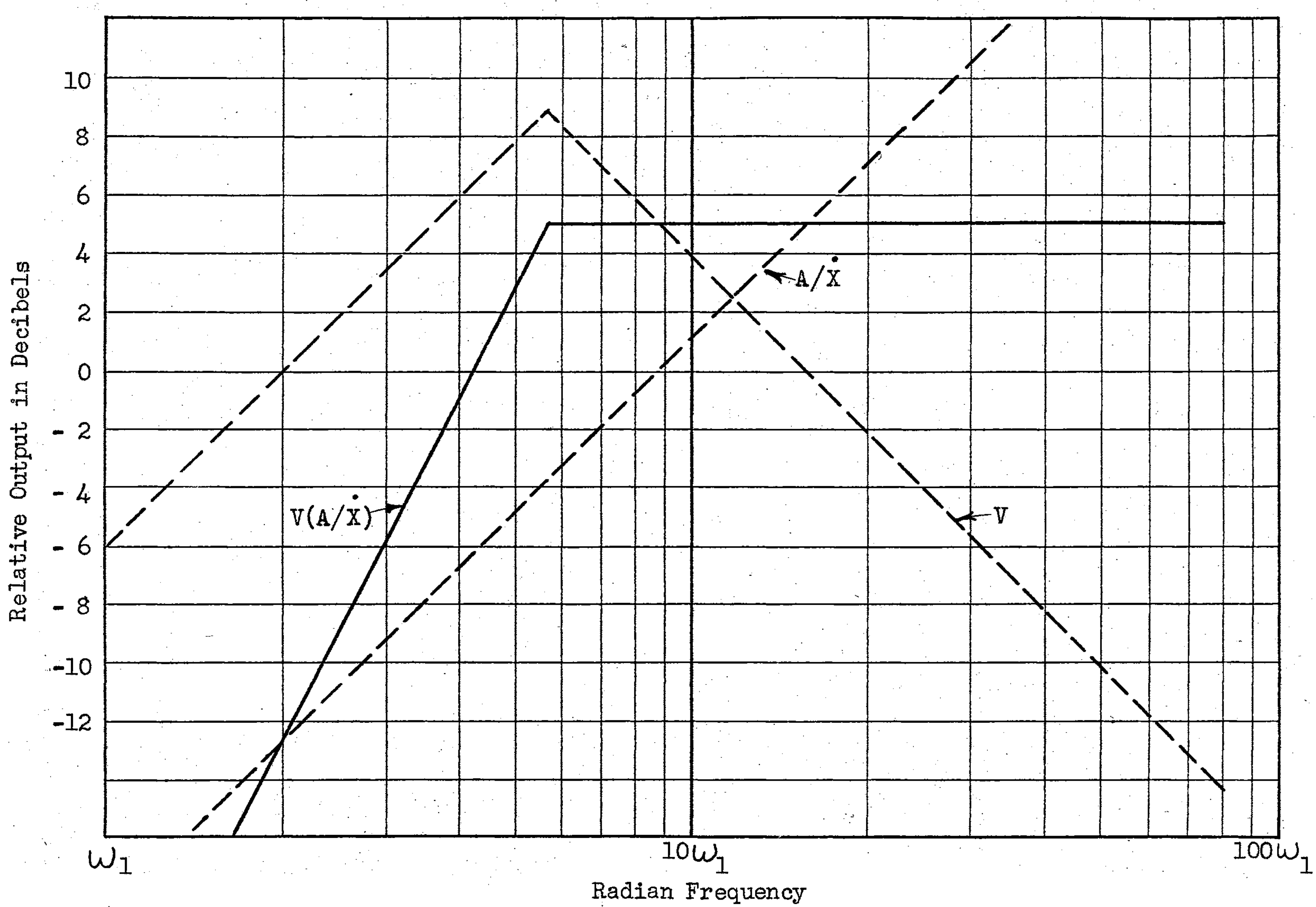

Curve 4. Bode Plot of the Speaker Transfer Function, V(A/Ẋ).

CHAPTER III

OPEN LOOP RESPONSE

The approach to open loop response measurements is of vital importance. The decision for or against indoor operation of the electro -acoustical device seems to warrant close consideration. While it is certainly true that the performance of a permanently installed system would be within the confines of a room, complications arise, however, due to room acoustics and speaker loading. It would, perhaps, be sufficient to define a standard room having certain dimensions and absorption characteristics. The difficulty in this approach lies in the fact that seldom, if ever, would the average listener be able to provide just such an environment. Thus, the inclusion of standard room acoustic data would be an additional item of complication in the description of system performance.

The most satisfying data obtainable will be that generated in an infinite space region. The result will be a display of the characteristics of the transducer alone and provides a means for a comparison of the relative performance of these units.

In order to insure the measurement of these characteristics, the speaker of this study was placed in free suspension above the roofs of surrounding buildings, thus tending to minimize reflection effects. Plate I illustrates this suspension. A 30 inch by 30 inch

PLATE I

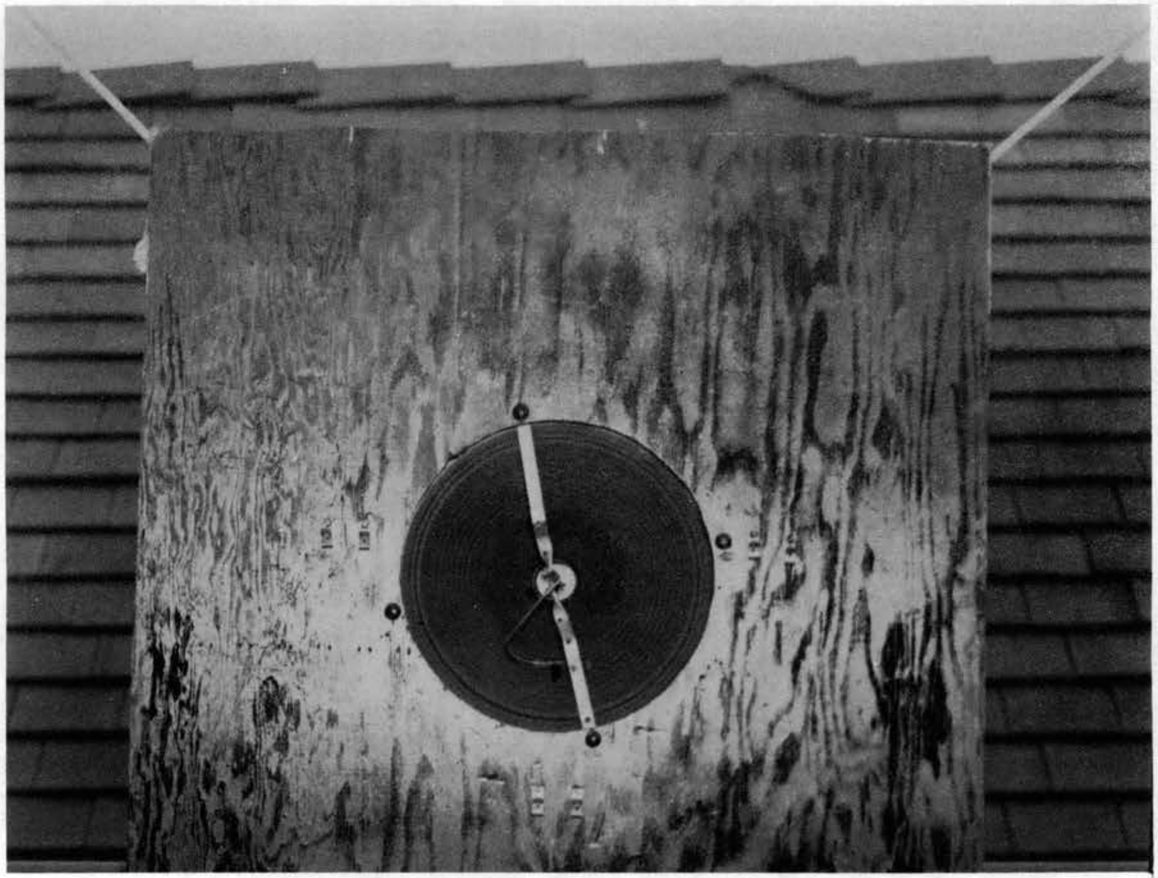

The Speaker and Baffling in Free Suspension.

baffle was added in an effort to emphasize the distinct resonant point below 100 cycles per second.

Figure 6 is a schematic of the test circuit. The oscillator and power amplifier are Heath Kit Models AG-10 and W-6M respectively. The sound-level meter (Type 1551-A) is a product of General Radio Company. This meter was located five feet from the apex of the cone. Such proximity was desirable so as to keep the direct to reflected output ratio at a maximum. A closer location would have resulted in wave cancellation (14) at some frequencies due to the cone shape of the speaker and was deemed undesirable.

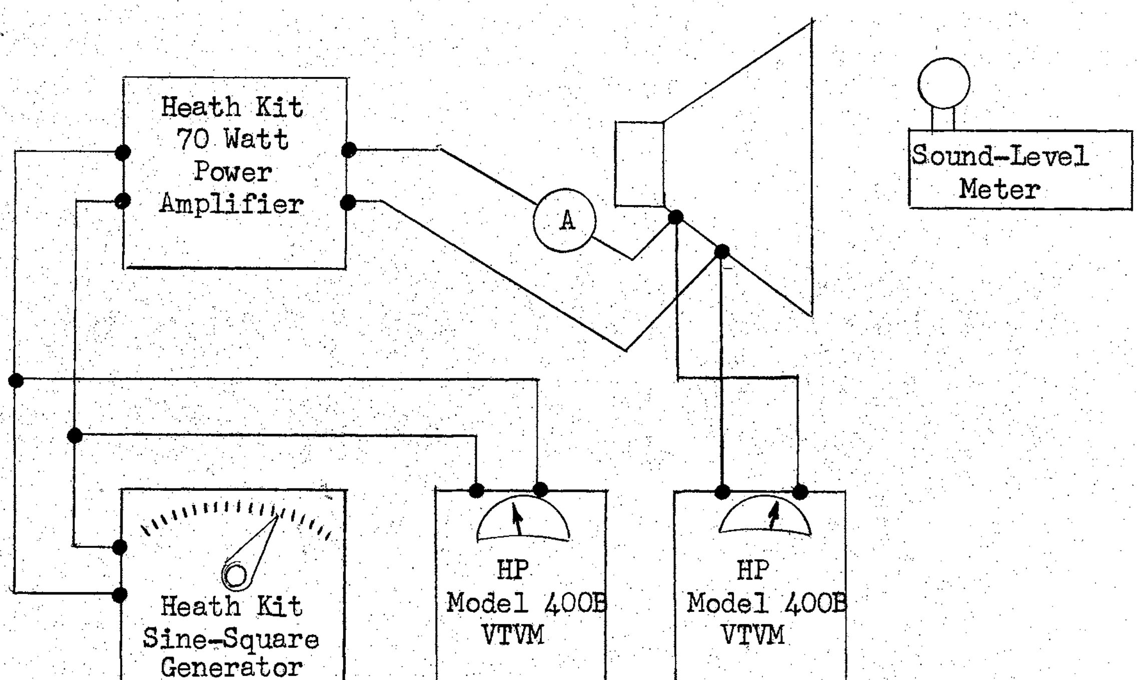

Figure 6. Open Loop Frequency Response Test Circuit.

The equipment of Figure 6 appears in Plate II. Data from the use of this apparatus is located in the Appendix under the title, "Open Loop Response Data." Curve 5 depicts the open loop system response in terms of decibels. Such a plot should not be confused

PLATE II

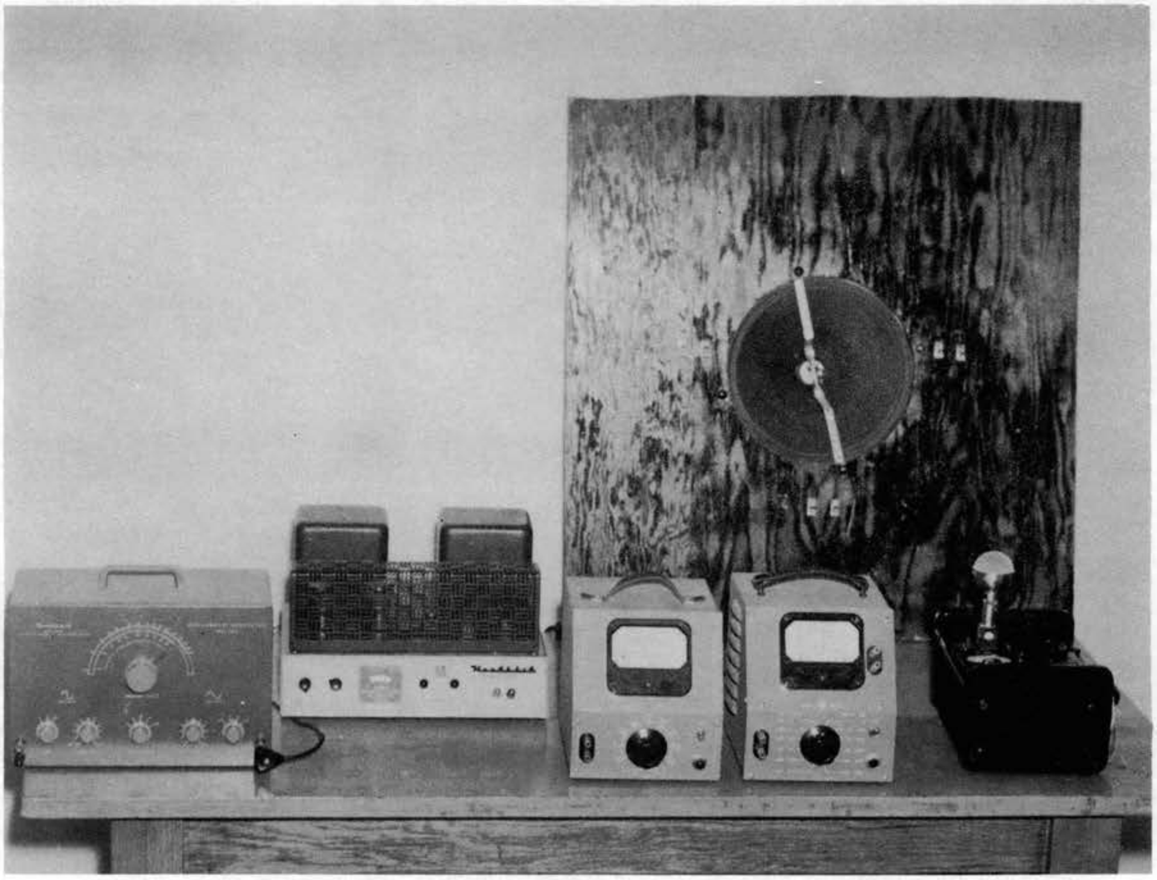

Open Loop Frequency Response Equipment.

with the gain characteristic of Curve 6, since for the first of these two plots the decibel is taken with reference to a 0.0002 μbar pressure level and no indication of the input is made. On the other hand, Curve 6 has been constructed to illustrate the decibel gain of the entire amplifier and speaker combination. This was accomplished by using equation (23). (15).

$$db = 20\log_{10} \frac{P_o}{V_{in}} \qquad (23)$$

where:

P_o = the absolute value of pressure output

V_{in} = the input voltage to the amplifier (250 mv)

Numerical results of the computations are listed as "Decibel Gain Computations for the Open Loop Frequency Response" in the Appendix.

Relative response data were taken on two speakers. The transducer characteristic described by Curves 6 and 7 are for a Jensen 12 inch speaker. Curve 8 shows the open loop frequency characteristic of a Heath Kit 12 inch replacement speaker. A comparison of Curve 6 with Curve 8 indicates much similarity between the general shapes of the plots. An analysis of other types of speakers would still reveal the same general shape. The discussion of the modification of the output by closed loop methods in succeeding chapters will apply to any transducer of this same general design. The essential difference from one system to another lies only in the frequency and gain at which resonance occurs.

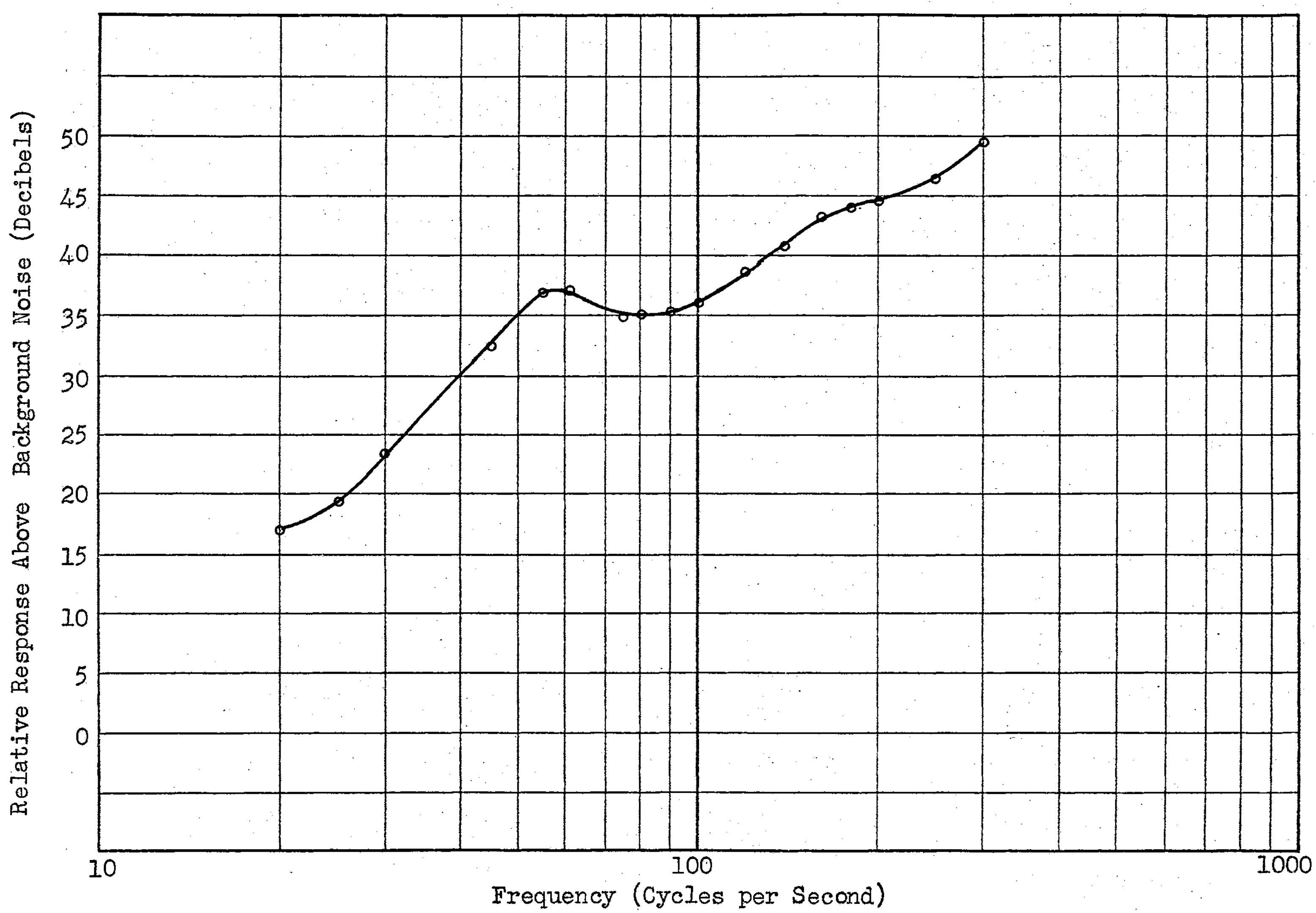

Curve 5. Open Loop Frequency Response of Jensen 12 Inch Speaker.

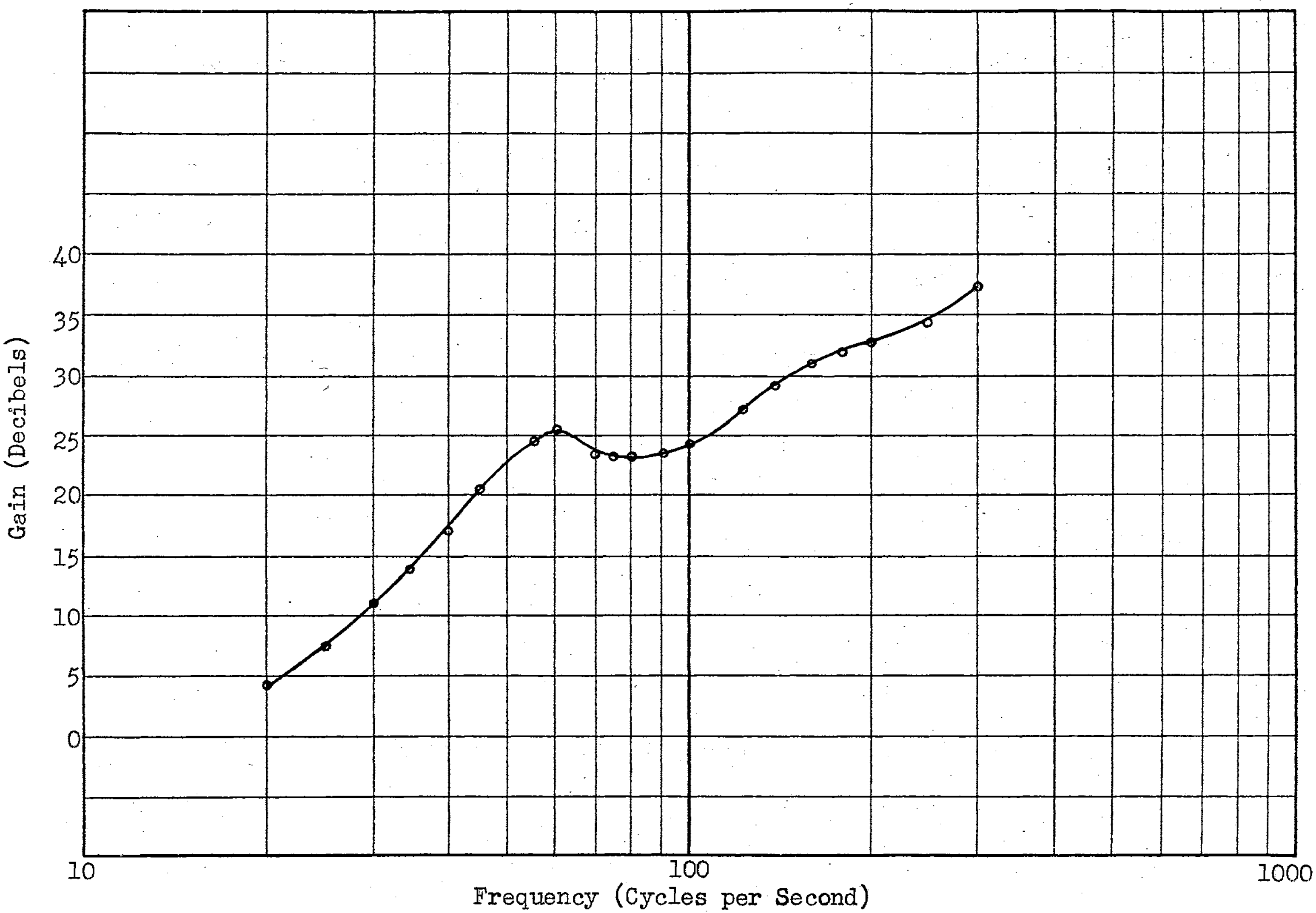

Curve 6. Amplifier-Speaker Frequency Response.

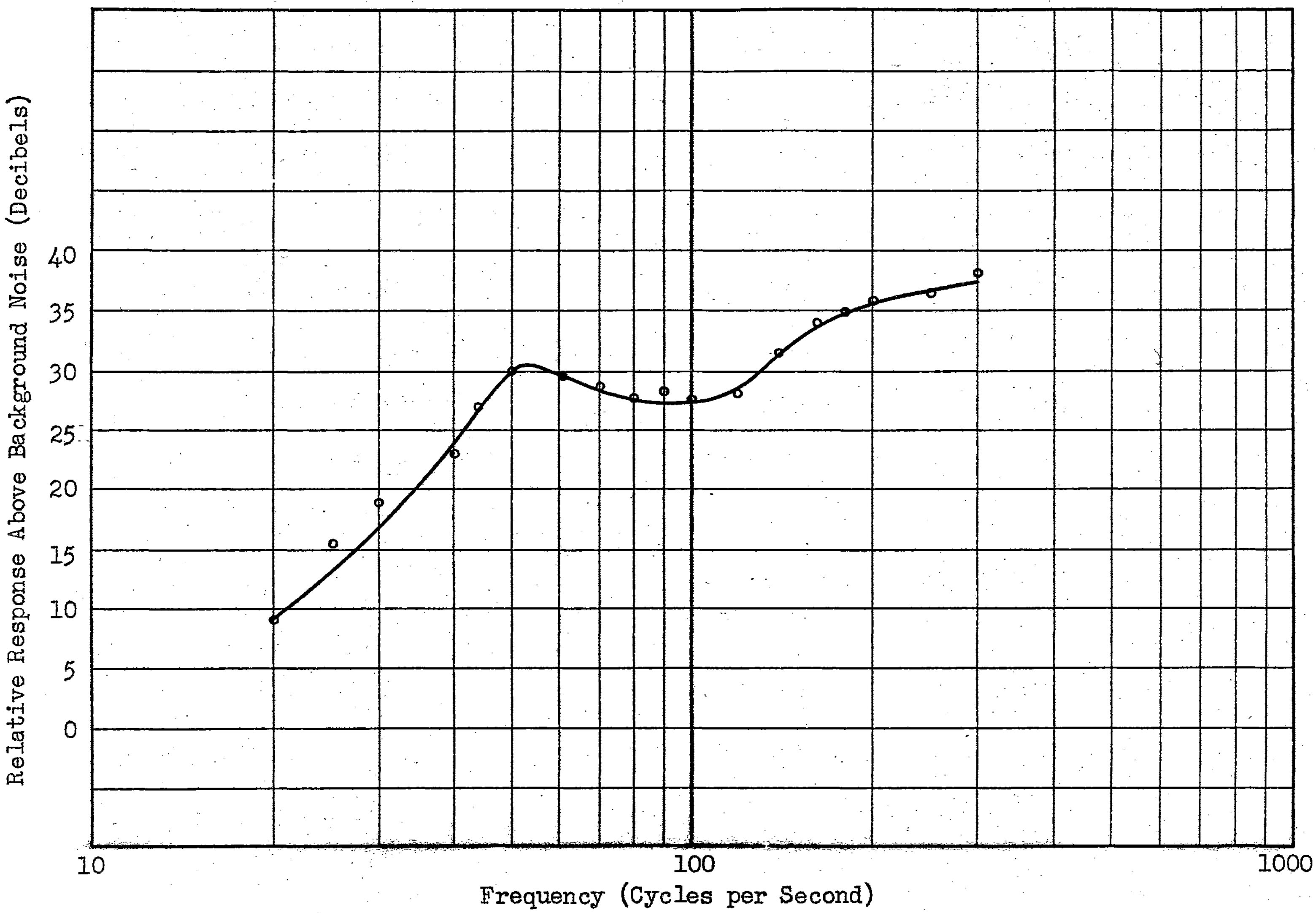

Curve 7. Open Loop Frequency Response of Heath Kit 12 Inch Replacement Speaker.

CHAPTER IV

CLOSED LOOP DESIGN CONSIDERATIONS

The Selection of A Velocity Transducer

The curves of Chapter III have been presented for a particular purpose. An improvement in characteristics is detectable only by comparison of these plots with the final closed loop response. Before such a comparison may be undertaken, the closed loop system must be synthesized and designed.

The determination of components for the operation of the speaker as a servomechanism created several interesting problems. The first step was the selection of the output transducer. The many requirements created complexities of no small magnitude. It was desirable, for instance, that the transducer indicate speaker velocity without changing its velocity characteristics to any great extent. Since a mechanical connection has to be established between the speaker cone apex and the transducer, the latter must have low mass and friction as well as high compliance. It was also very necessary that the transducer's electrical output impedance be held to a minimum. This requirement arose from the fact that the speaker (and therefore the transducer) was not in close proximity with the amplifier. Low impedance circuitry tended to minimize 60 cycles per second noise voltages induced in the return line thus yielding a high signal to noise ratio.

In addition to these features a high degree of linearity was needed. Finally, it was important that the transducer accept translational motion signals as an input.

The Sanborn LVsyn linear velocity transducer was found to meet the above specifications satisfactorily. This instrument has an internal resistance of 1000 ohms and an inductance of less than 0.0045 henries. The mass of the moving section was 3 grams. Plate III shows the model 3LVA5 that was actually used.

Protruding from the right end of the housing is a magnetic core. Any motion of this core inside the stationary coil of the housing produced approximately 102 millivolts per inch per second of output. The attachment of the magnetic core to the cone apex was made by means of a threaded aluminum extension rod, while the housing was secured in front of the speaker by means of an aluminim bracket. See Plate IV.

In order to be certain of negligible changes in the characteristics, a rerun of the speaker's frequency response was made. The results are displayed as Curve 8 and appear in tabulated form in the Appendix. A close comparison of this plot with that of Curve 5 indicates little change, although a slight decrease in response amplitude was experienced.

The next item of interest in the closed loop evolution is the measurement of cone velocity as a function of frequency. Curve 9 depicts the velocity (measured as transducer output voltage) of the speaker in ratio to the amplifier input voltage. Curve 10 is the asymptotic approximation of Curve 9. This will be the curve used throughout the synthesis and design to represent the function K x V.

The terms K and V imply the same quantities here as in Figure 5. Since the amplifier is extremely wideband in nature, the plot of K x V is in essence a proportional plot of V.

Curve 3, Y(S) versus frequency, was a prediction of the low frequency velocity characteristics of the cone. Much similarity exists between this curve and those of Curves 9 and 10. The slight discrepancies in the higher frequency regions arise from the inaccuracies of the assumptions made in deriving Curve 3. There the cone was considered to move as a unit, when in fact its motion at higher frequencies is a much more elaborate function. Various modes of vibration are established due to the compliances which were here-to-fore considered negligible.

Closing The Loop With Velocity Feedback

From these data it is now possible to develop a degenerative feedback loop control system. Two of the many such systems are to be considered. The first of these is direct velocity feedback and the second a compensated velocity feedback system.

The design work is conducted with the aid of the Bode asymptotes. In order to illustrate the use of these straight line approximations, consider a system with an open loop transfer function of KV(S). The output from KV(S) is fed back to its input through a function, β(S). The feedback signal, along with the system input signal is summed in a negative fashion. The overall transfer function of the system then becomes

$$\frac{\Theta_o}{\Theta_i} = \frac{KV(S)}{1 + \beta(S)KV(S)} \quad . \qquad (24)$$

PLATE III

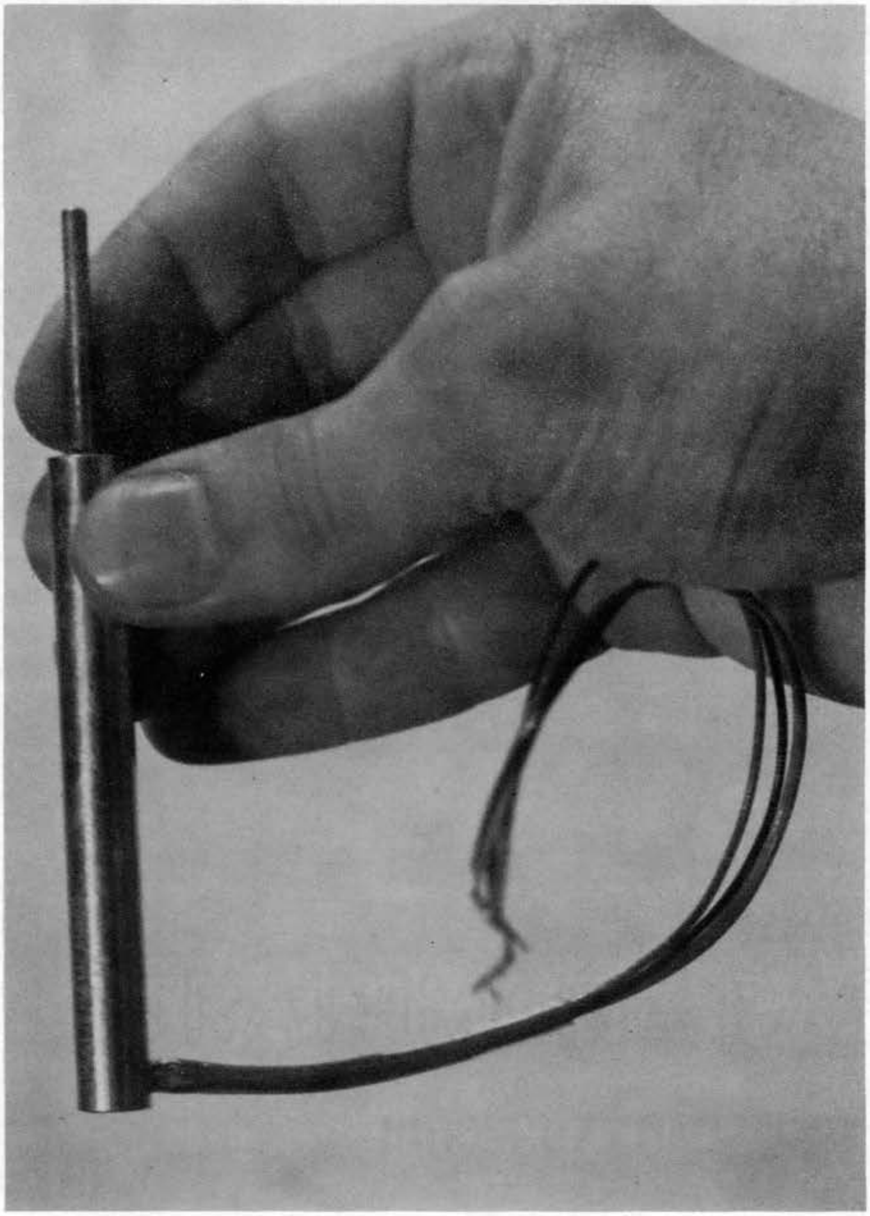

Model 3LVA5 Sanborn Linear Velocity Transducer.

PLATE IV

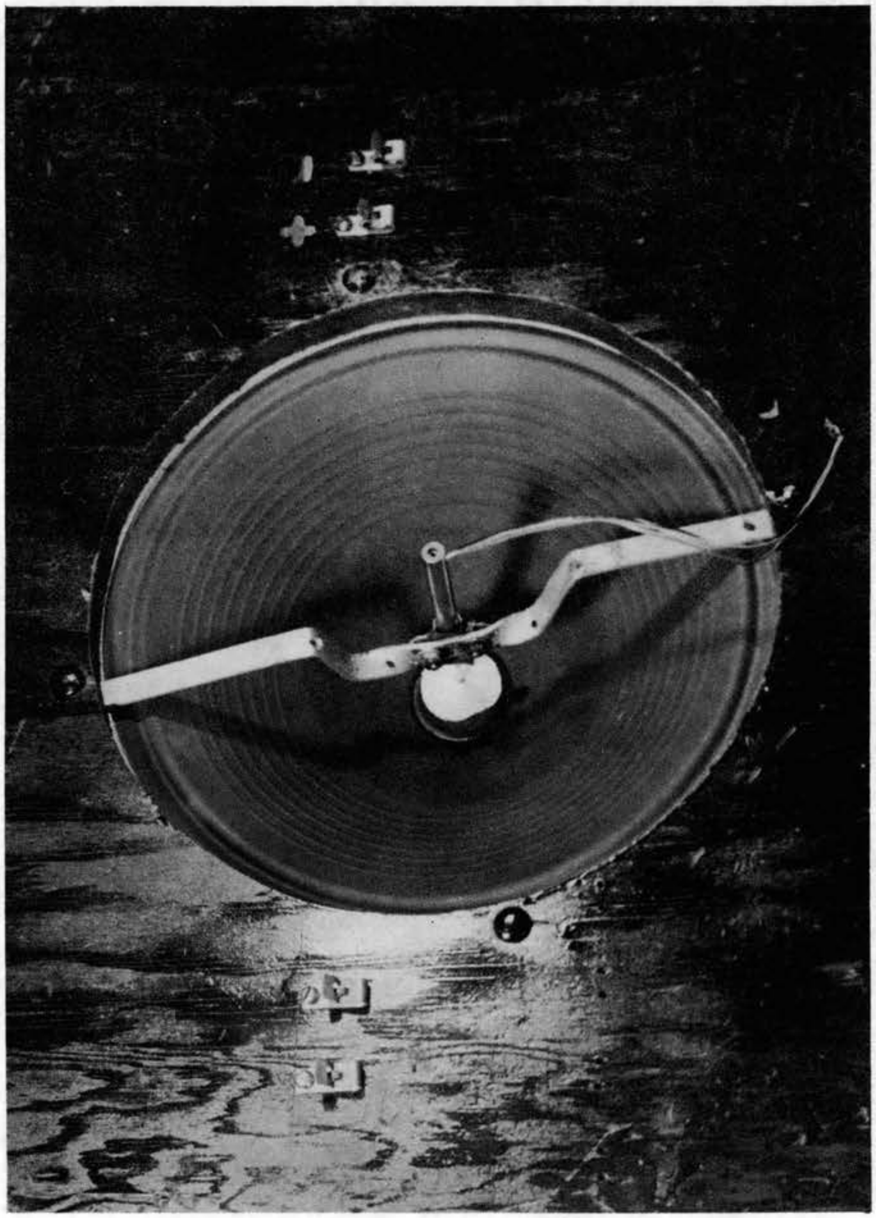

Mounting Arrangement of the LVsyn Linear Velocity Transducer.

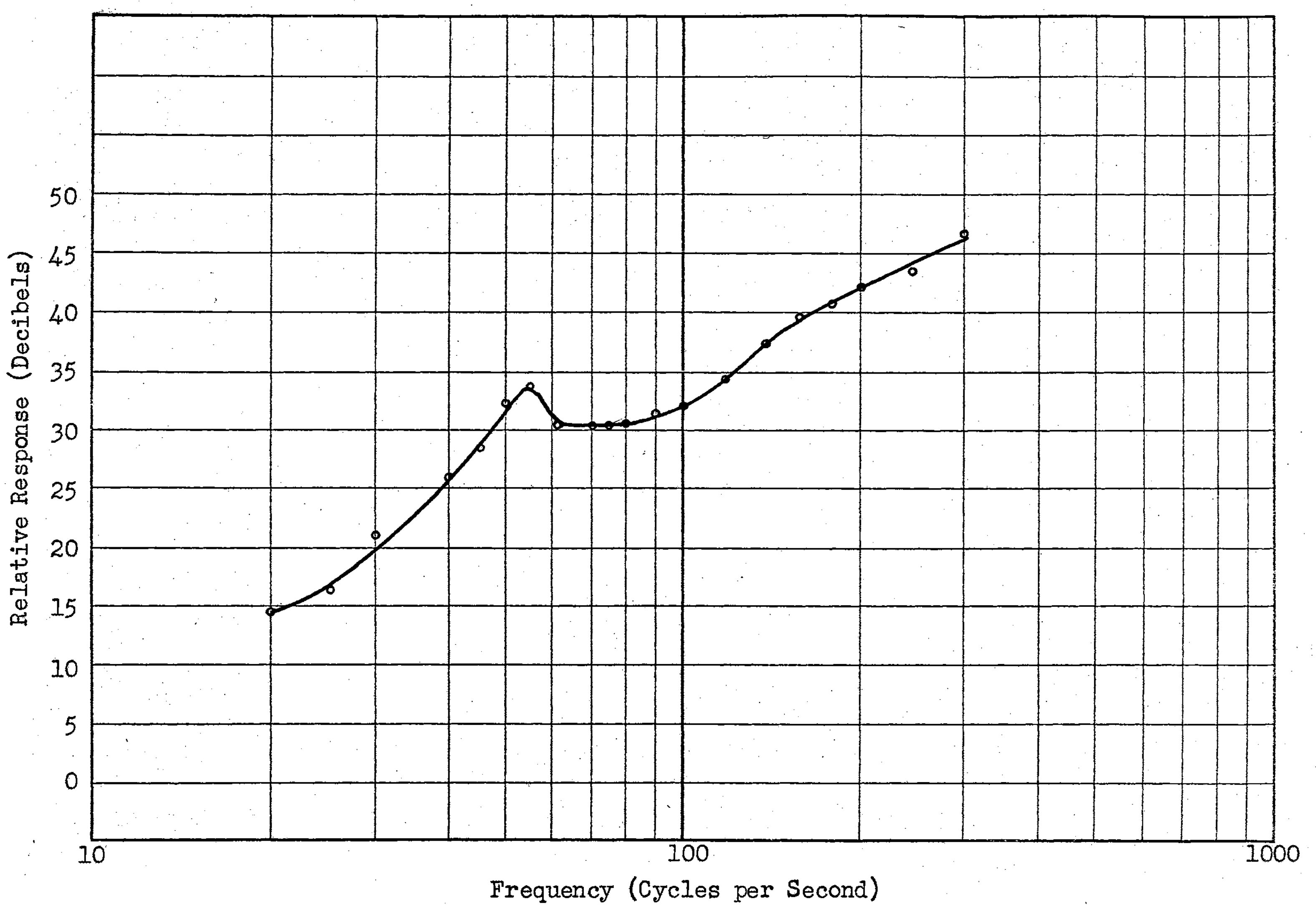

Curve 8. Open Loop Frequency Response of Speaker and Sanborn Velocity Transducer Combination.

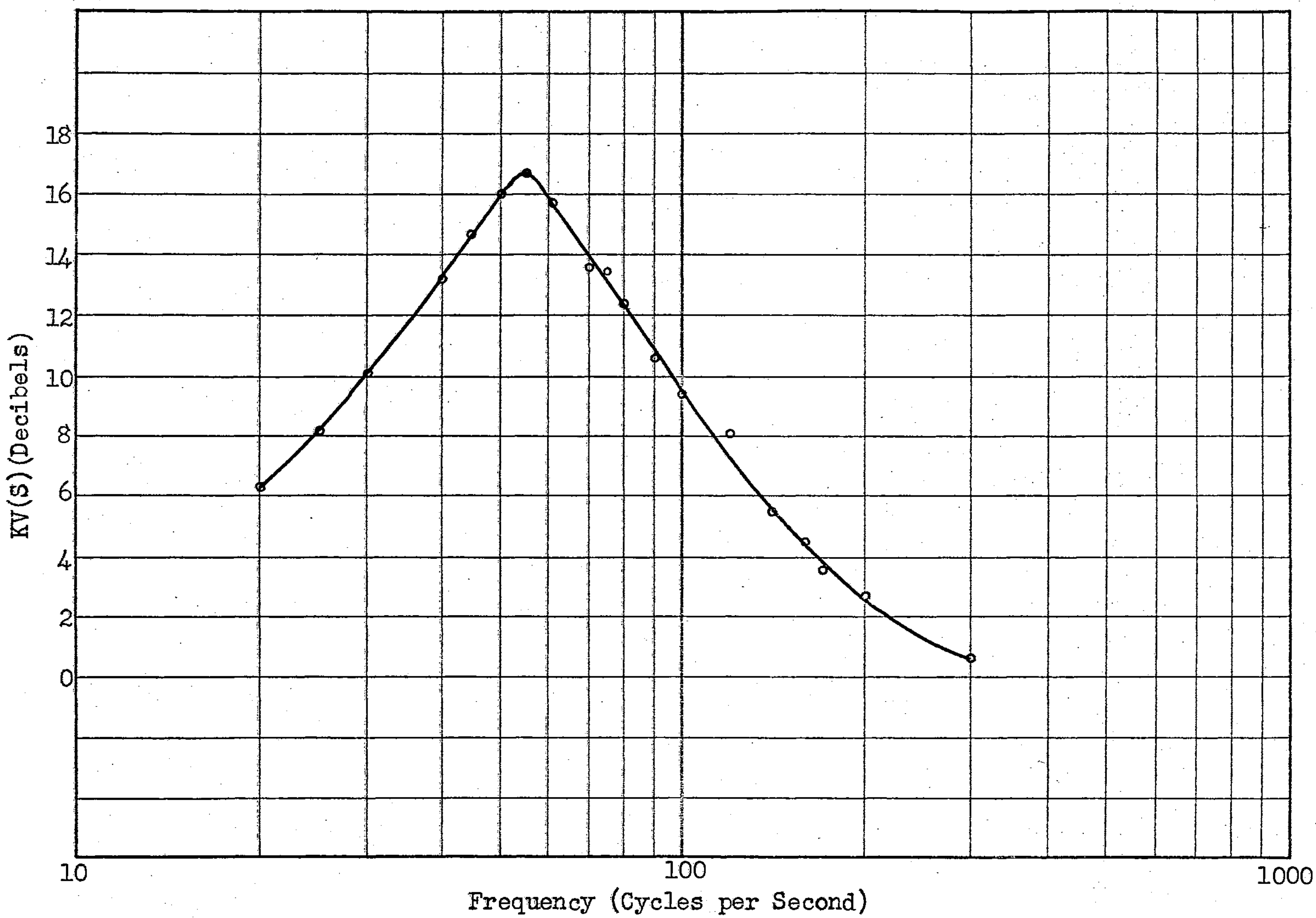

Curve 9. Experimental Velocity Transfer Function Frequency Response.

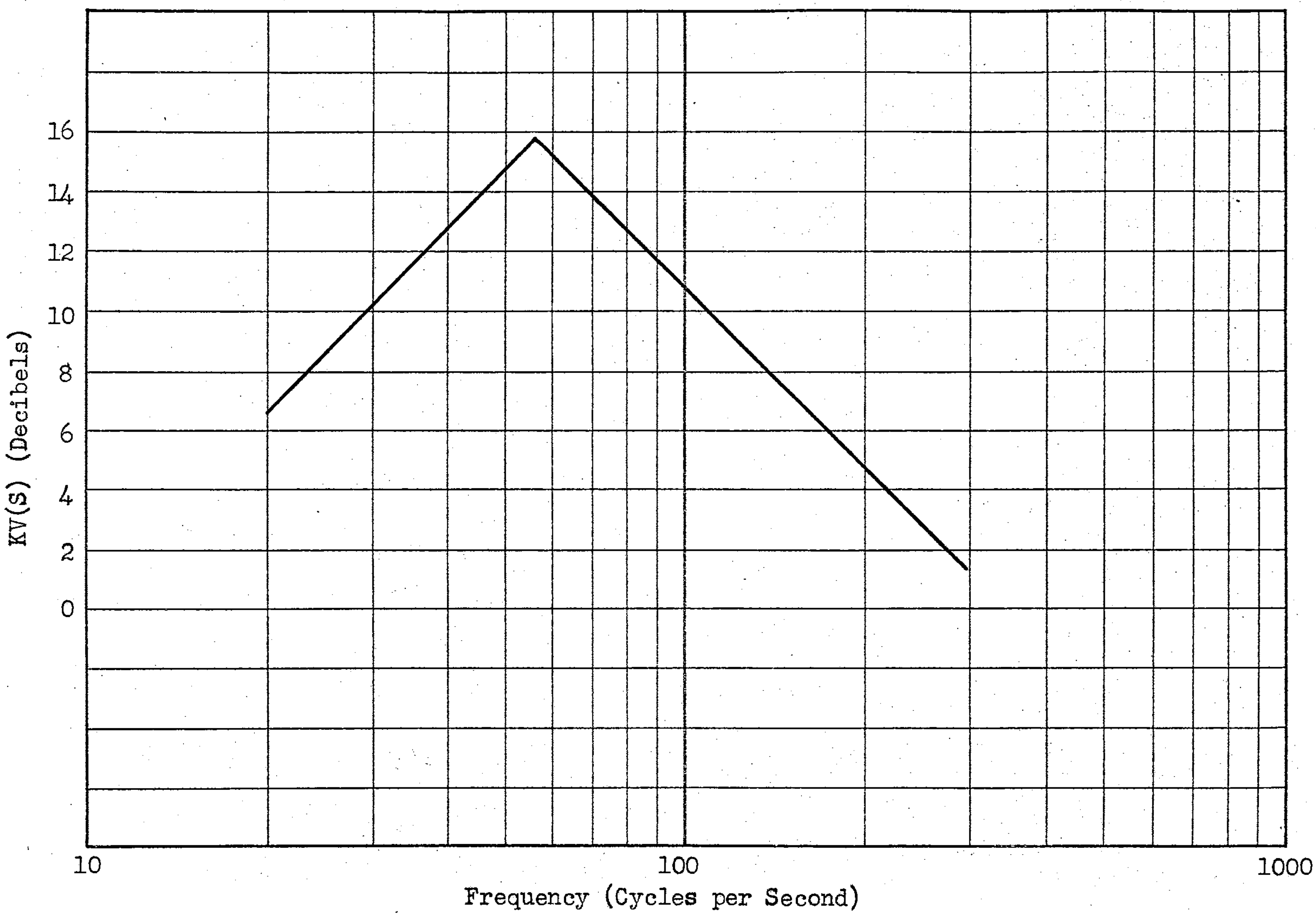

Curve 10. Asymptotic Approximation of Curve 9.

Investigation of the steady state sinusoidal response as the frequency is varied leads to several approximations that are invaluable in executing an approximate graphical solution. Let KV(S) be very small compared to unity. This obviously justifies the assumption

$$\frac{\Theta_o}{\Theta_i} \approx KV(S) \tag{25}$$

Under many normal situations, as is the case of this study, KV(S) will be small at low frequencies as well as high. In between these two regions lies an area in which KV(S) is very large when taken in comparison to unity. Under these circumstances

$$\frac{\Theta_o}{\Theta_i} \approx \frac{1}{\beta(S)} \; . \tag{26}$$

Now, if a curve of KV(S) were drawn, and on the same sheet a plot of $1/\beta(S)$ was made, the total function Θ_o/Θ_i could be obtained (approximately). For very small values of KV(S) the overall gain will follow the curve of KV(S). This is also true for high frequencies. In between, the $1/\beta(S)$ curve will approximate the system response. Some error develops around the cross over points from KV(S) to $1/\beta(S)$ and back to KV(S). These errors are relatively unimportant and will be neglected in the forthcoming analysis.

Let attention now be given to the direct velocity feedback case. The ultimate goal of this attention is to de-emphasize the 57 cycle per second resonant point and produce a flatter response. For direct velocity feedback, β is assigned a constant value. The gain of β must be restricted to 0.5 or less since, from phase shift considerations, the system is unstable (sustained or growing oscillations) for values greater than this. It is also true that the controlled velocity is actually the input to another function $A/\dot{X}$. The overall improvement can be obtained only by taking

$$\left[\frac{KV(S)}{1 + \beta KV(S)}\right] \bullet \left[G(S)\right] \tag{27}$$

where

$$G(S) = \frac{A}{\dot{X}} \quad . \tag{28}$$

It becomes necessary to calculate the value of $A/\dot{X}$. Curve 11 demonstrates this computation. The top dashed plot is KV(S)G(S) while the lower curve represents -KV(S). Addition of these plots produces

$$\frac{KV(S)G(S)}{KV(S)} = G(S) \tag{29}$$

which is shown as a solid line and will be called the decoupling function. This function is unchangeable for constant radiation area, shape and surroundings.

The application of negative feedback to the speaker-amplifier combination is accomplished with the aid of Curve 12. The solid line plot is the asymptotic response,

$$\frac{\Theta_o}{\Theta_i} = \frac{KV(S)}{1 + \beta KV(S)} \quad . \tag{30}$$

Multiplication of this function by G(S) produces the closed loop acoustic characteristic illustrated by Curve 13.

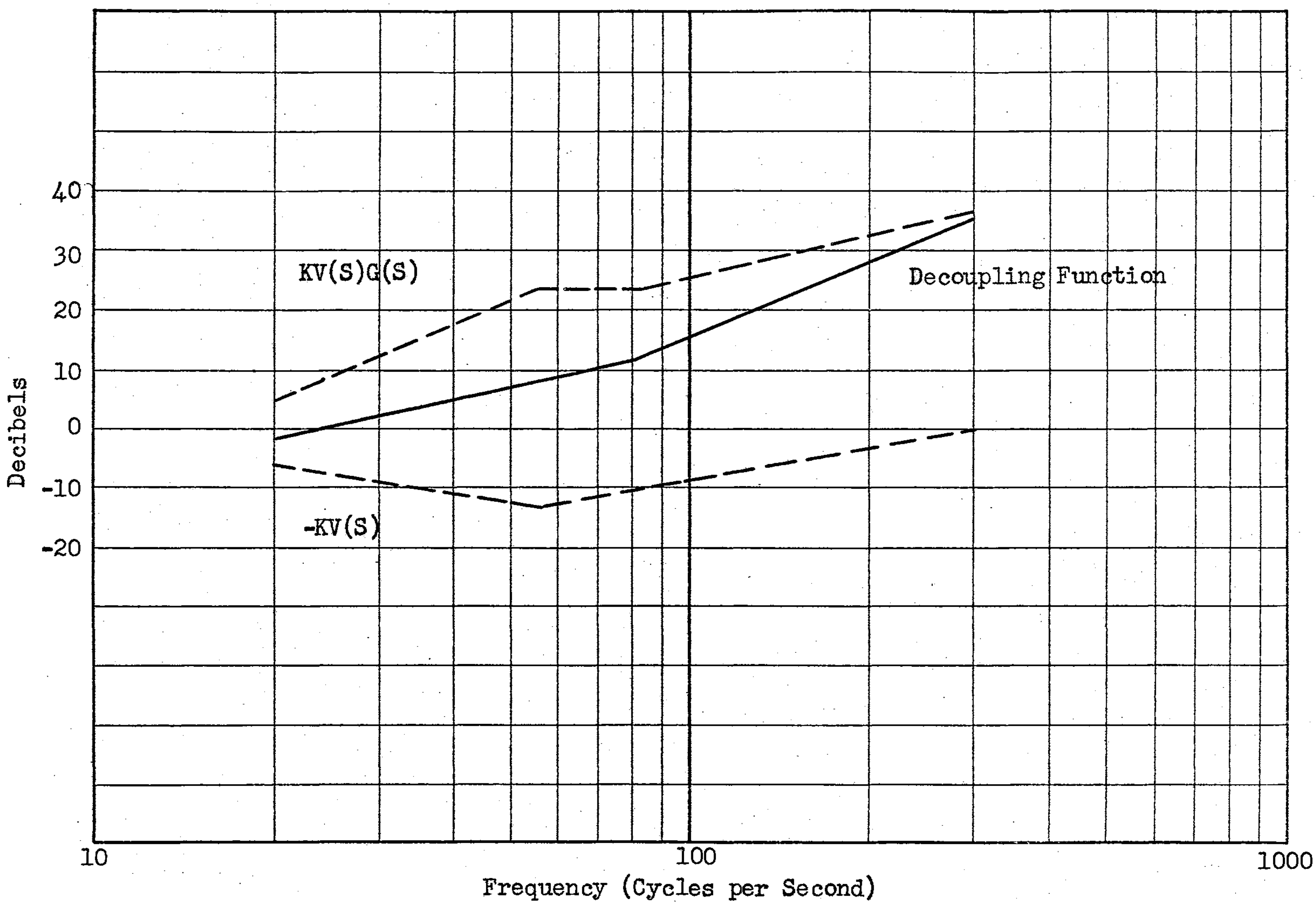

Curve 11. The Calculation of the Decoupling Function, G(S).

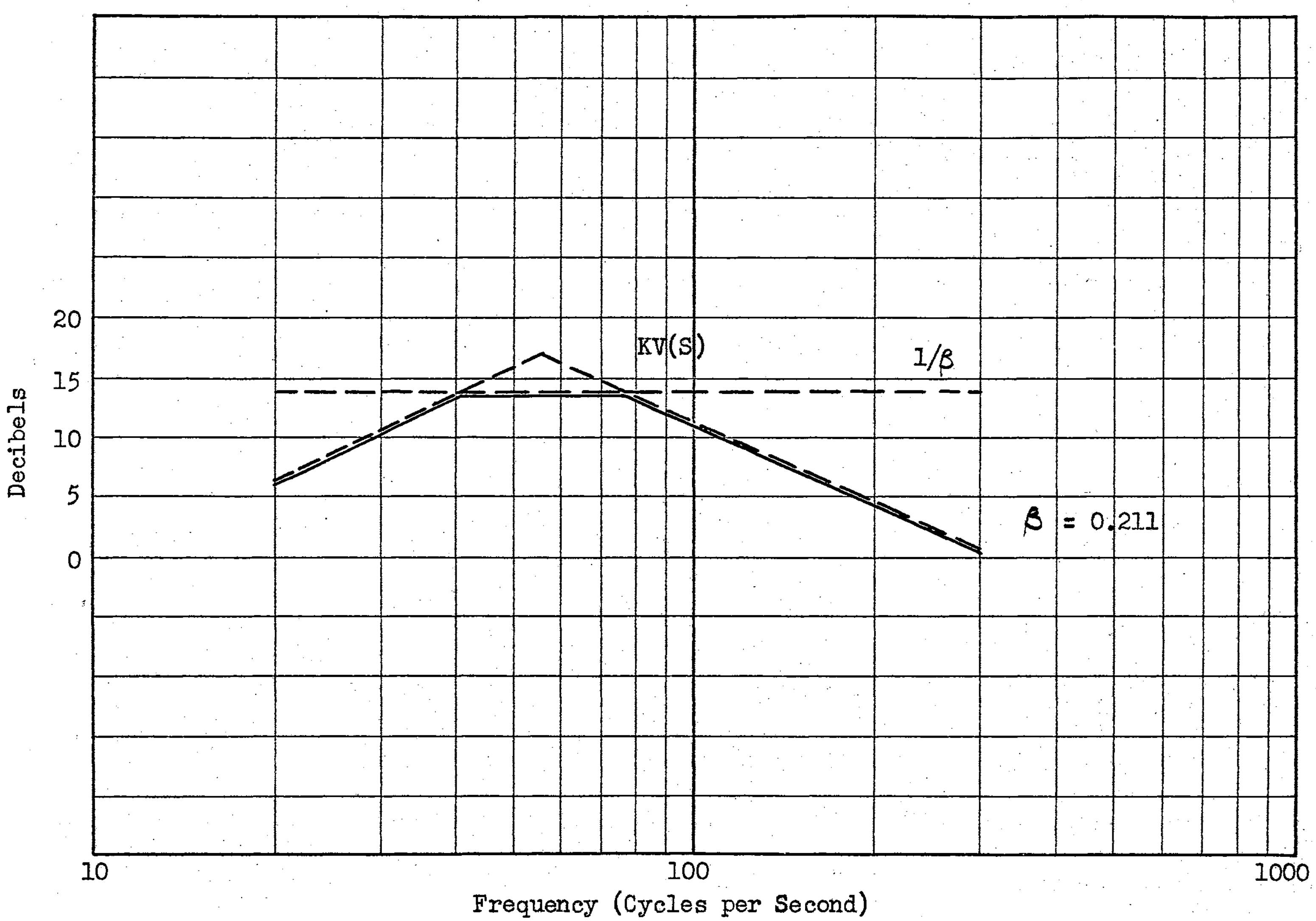

Curve 12. Calculation of Closed Loop Velocity Response.

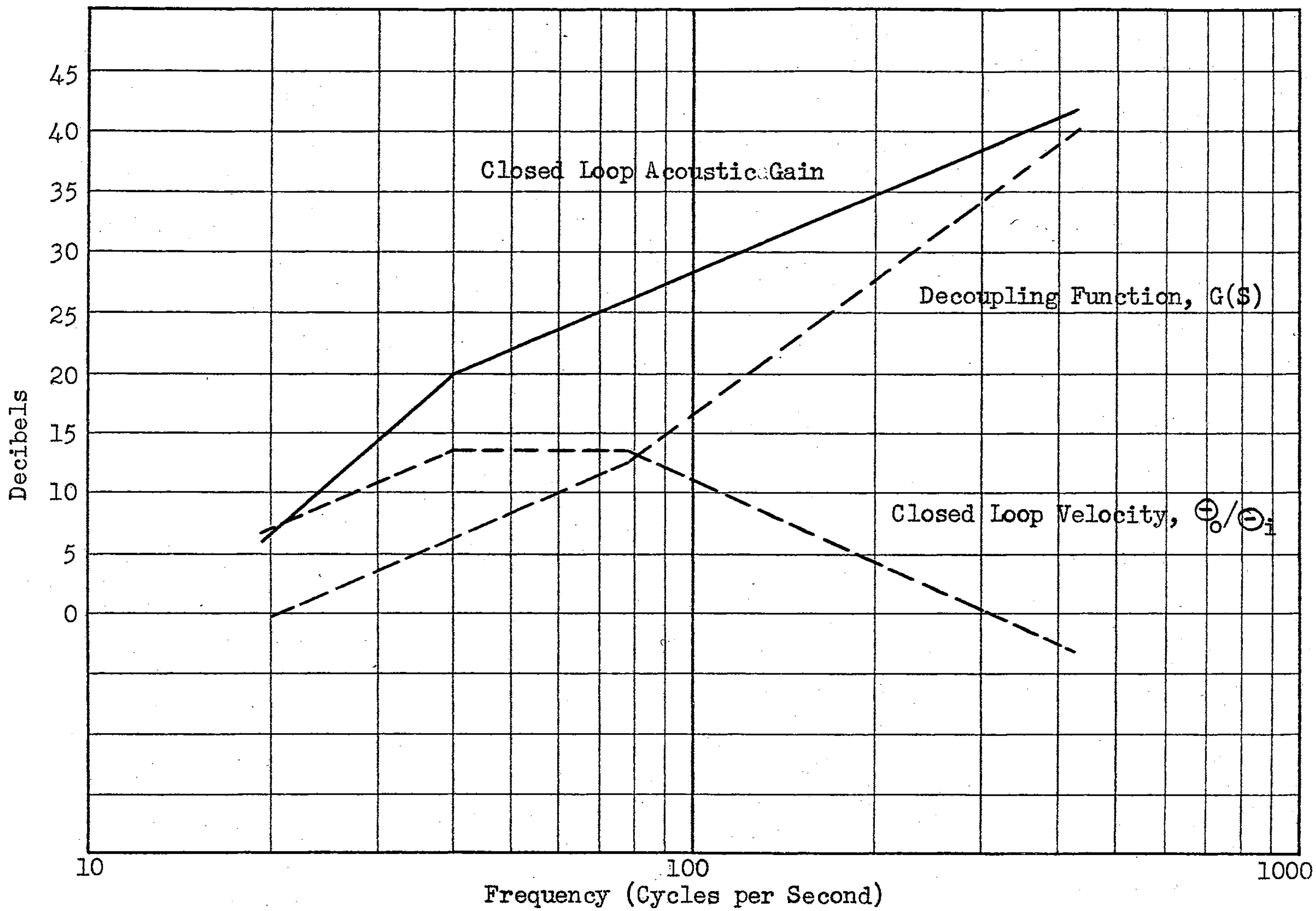

Curve 13. Computation of (Θ_o/Θ_i) G(S) .

Note that this response is considerably more uniform than the previous open loop curve and contains a single break frequency. It is also interesting to see that the point of slope change is lower than the original resonant frequency corresponding to a wider bandwidth for the speaker. This type of network, then, represents an improvement over previous arrangements but is far from the ideal case.

The Compensated Closed Loop System

A compensated response may be obtained in one of several ways. The function, β, may be incorporated as a frequency sensitive network. This would appear to be the most obvious method. Such an approach lends itself nicely to the graphical technique already mentioned but tends to require a $\beta(S)$ which is a derivative or phase lead circuit. Noise amplification in such a $\beta(S)$ makes this impractical. Also, the phase lead of $\beta(S)$ could contribute to instability. It would seem instead that forward loop compensation with a constant feedback velocity gain is the most suitable.

Curve 14 illustrates the final desired acoustic response. The overall gain has been sacrificed in order to achieve a flatter curve and more extended frequency band. There is absolutely no reason why this response in theory cannot be entirely flattened. Physical difficulties do develop, however. Such a curve would require low frequency velocities which are obtainable only through extremely large cone displacements. In reality, the motion is restricted to the region of the magnetic field. Large amplitude swings must be prevented because of the limited strength of the cone.

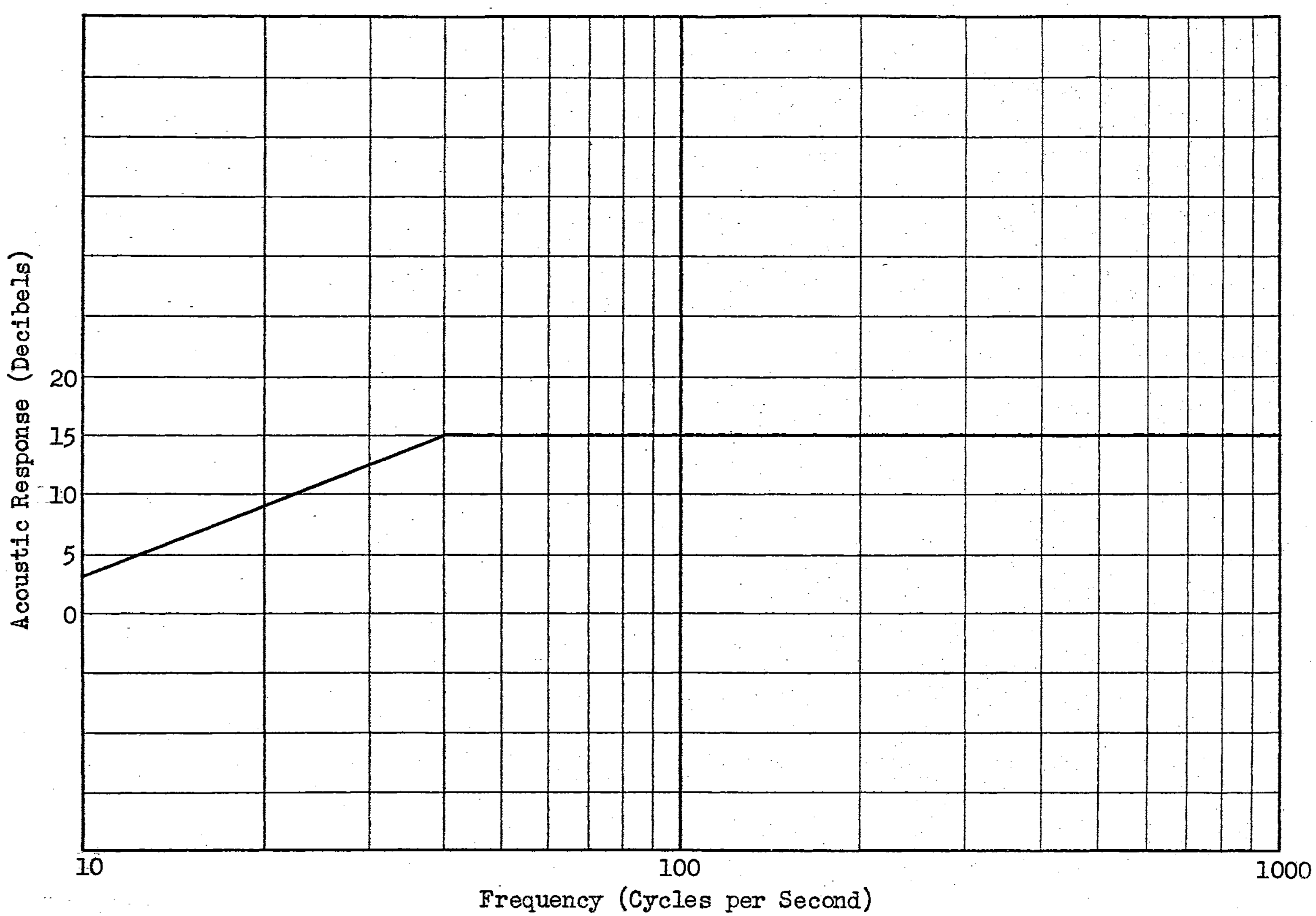

Curve 14. The Desired Acoustic Response.

If the system is to be compensated in the forward loop, let the compensating network have the transfer function, C(S). The equation representing the closed loop velocity control will then be:

$$\frac{\Theta_o}{\Theta_i} = \frac{KV(S)C(S)}{1 + KV(S)C(S)} \quad . \tag{31}$$

When Θ_o/Θ_i is multiplied by the decoupling function G(S) the result should be Curve 14. This, then, indicates that the division of the acoustic gain desired by G(S) results in the necessary plot of equation (31). This division is performed on Curve 15 and the solid line represents the result. The low frequency region points to a constant velocity gain. Since this is not possible, as mentioned earlier, a somewhat less ideal characteristic is accepted.

Suppose that a compensating network

$$C(S) = \frac{1}{(\tau S + 1)} \tag{32}$$

is cascaded with KV(S). If the appropriate value of τ is selected the function KV(S)C(S) will appear as in Curve 16. τ will be established by equation (33).

$$\tau = \frac{1}{2\pi f} \tag{33}$$

where

f = the frequency at which the negative 6 db per octave slope begins.

The application of constant gain feedback is illustrated by Curve 17. Comparison of this plot with the necessary controlled

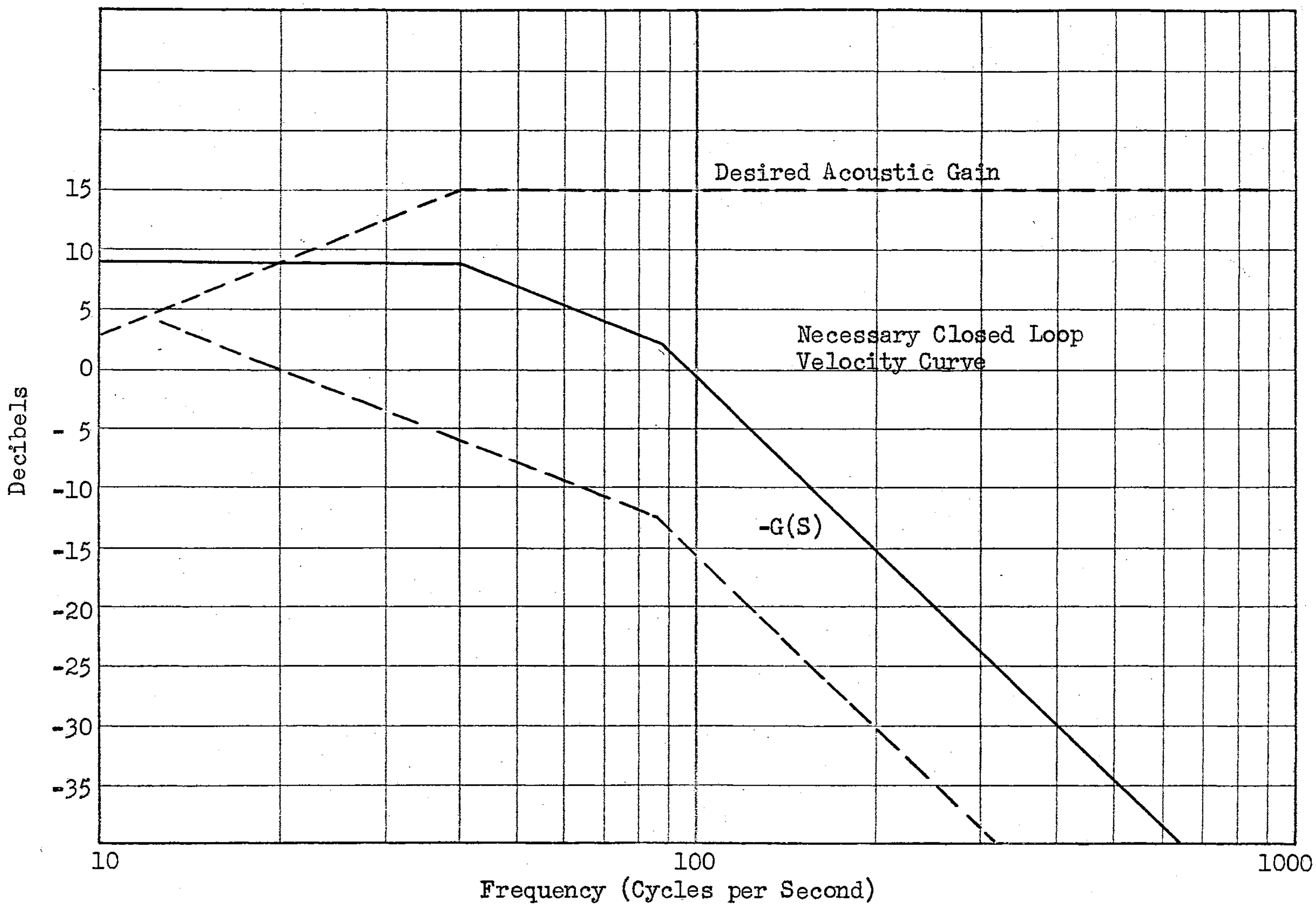

Curve 15. Calculation of the Necessary Closed Loop Velocity Curve.

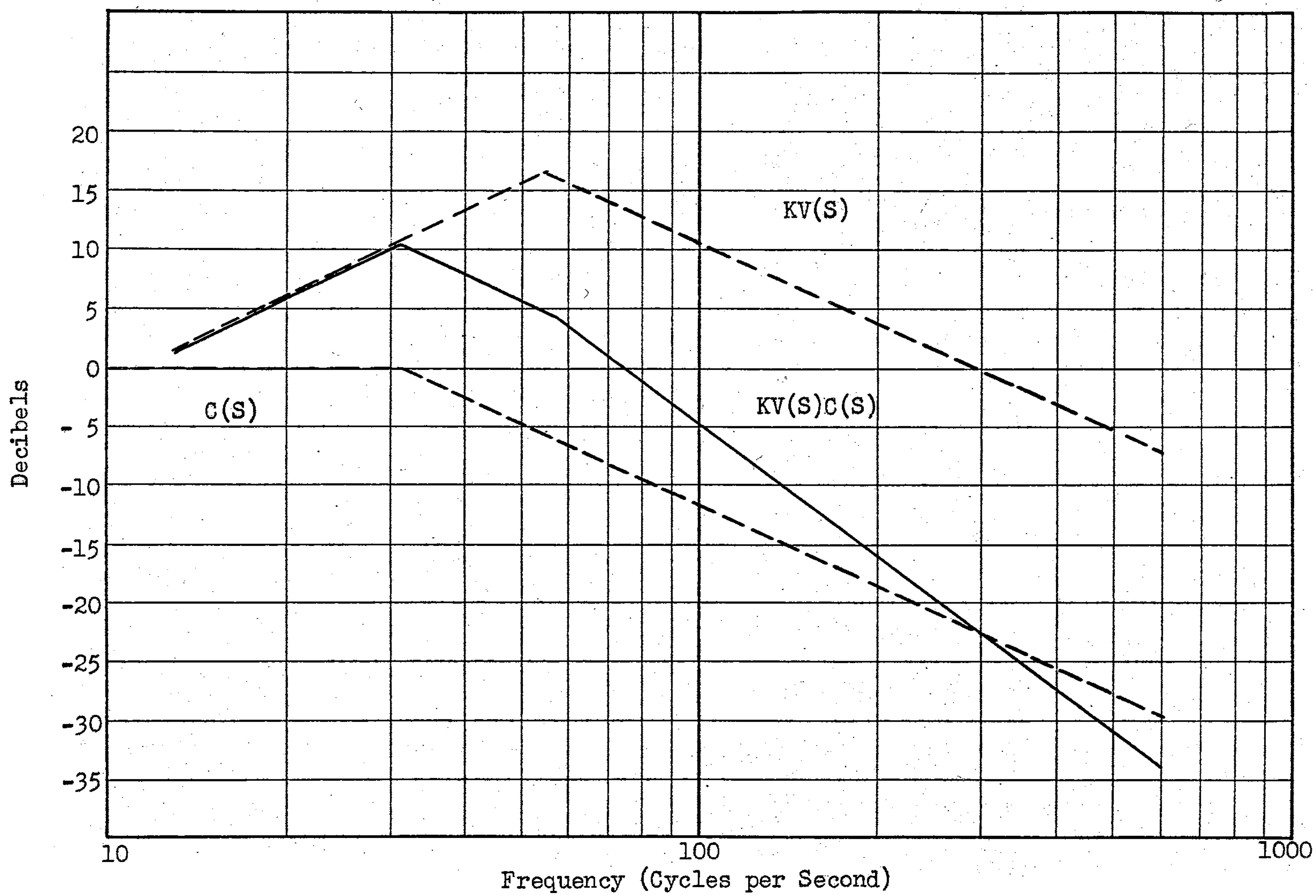

Curve 16. Determination of KV(S)C(S).

velocity of Curve 15 shows some difference although the shape is much the same. The relative ease with which Curve 17 may be obtained justifies further investigation of the overall acoustic gain using this function.

Moving in the opposite direction, the acoustic response may be calculated by the multiplication of Curve 17 and the decoupling function. See Curve 18. A gain plot of this nature is excellent. The extended frequency band and flattened curve have been virtually accomplished. In addition, the 12 db per octave attenuation in the range below 25 cycles per second tends to protect the speaker from excessive displacements.

The compensated closed loop response approaches the desired gain function and serves to illustrate that the closed loop system is far superior to any yet developed. At this point, it is recalled that the speaker baffle is a relatively small flat board. The next chapter will outline the physical realization of the control systems just described.

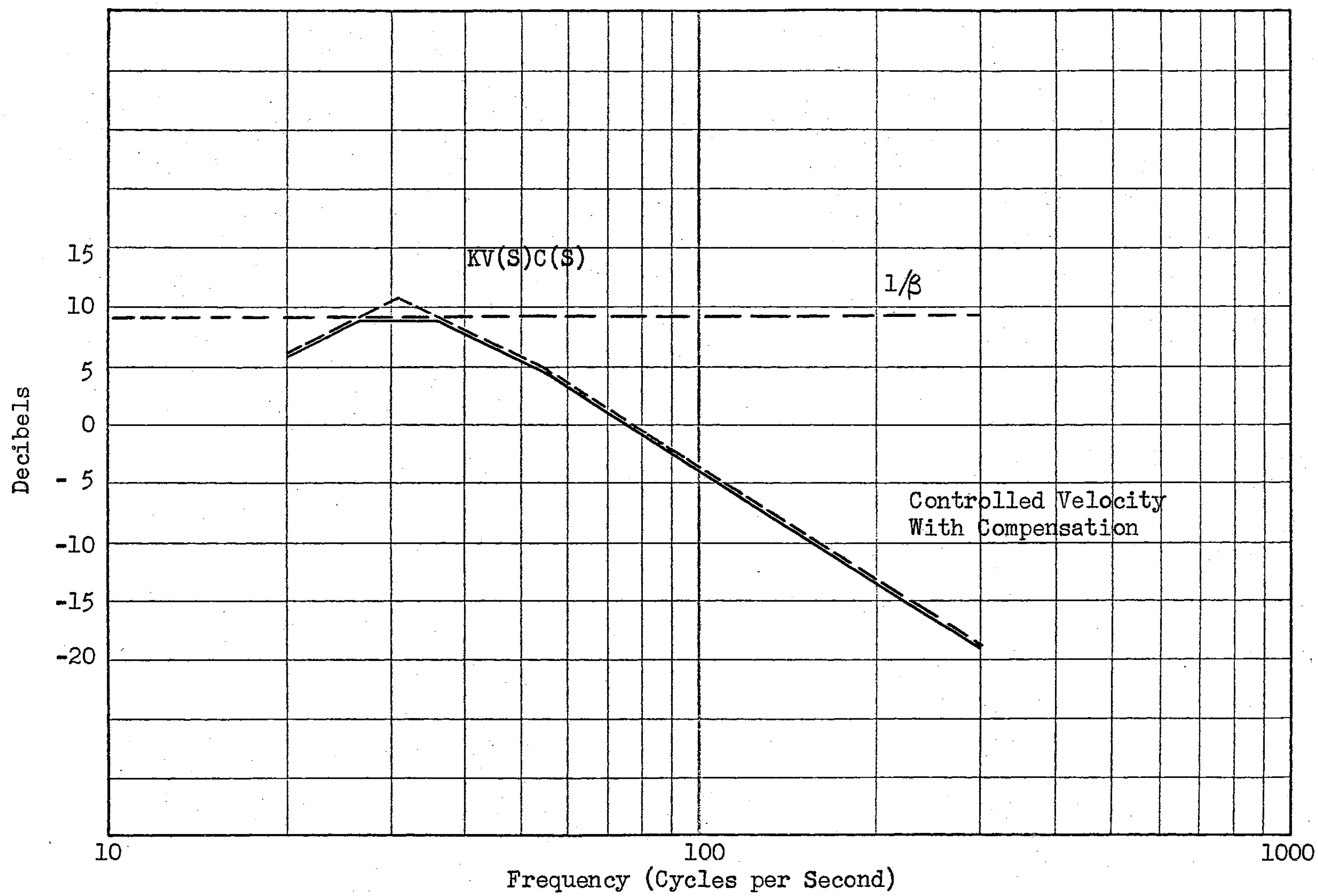

Curve 17. Application of Feedback to KV(S)C(S).

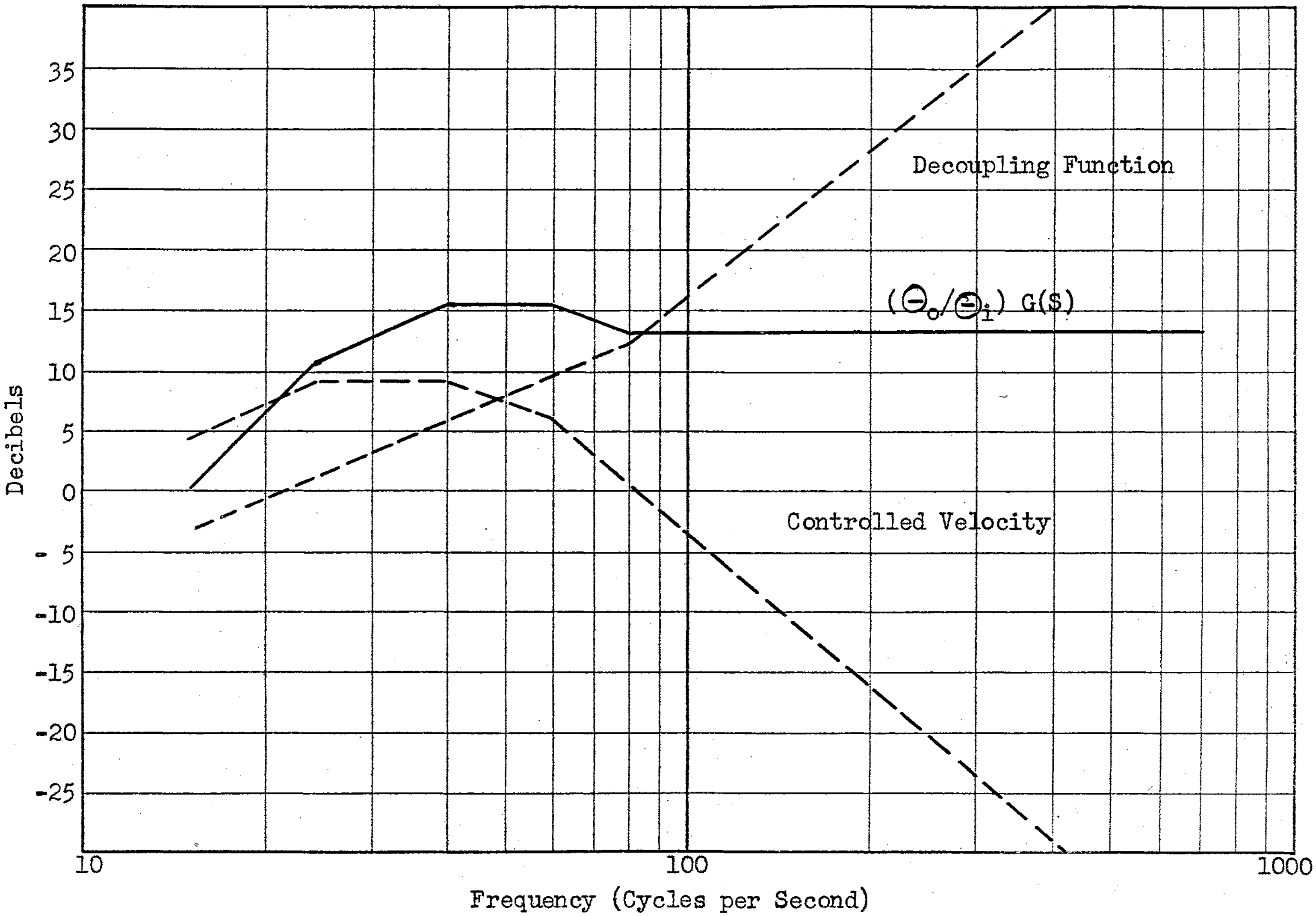

Curve 18. Compensated Acoustic Response.

CHAPTER V

THE DESIGN AND PERFORMANCE OF THE PHYSICAL CIRCUITRY

The Closed Loop Velocity Circuit

The final step in the development of this closed loop control system hinges around the physical realization of the synthesized transfer functions of the preceding chapter. Consider the case of direct velocity feedback. Figure 7 schematically represents this type of closed loop operation. Two of the items included in the

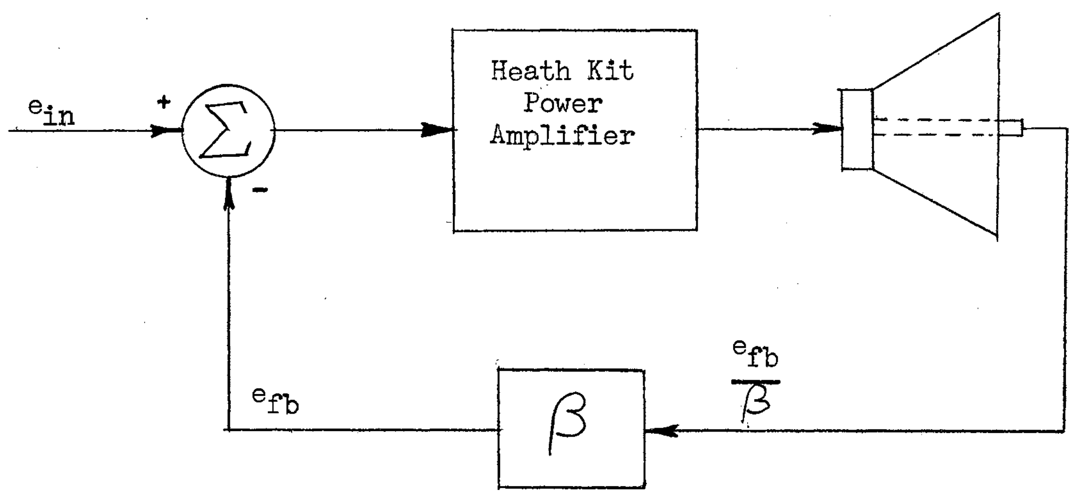

Figure 7. The Closed Loop Velocity System.

diagram are as yet undefined. The circle with a capital sigma (Σ) indicates a summing network. Conceivably this could be either passive or active in nature. In any finalized design, the passive network would feature many obvious advantages over the active variety.

Compactness and low cost are the most important of these, for the addition of two resistors to the existing grid circuitry of the Heath Kit power amplifier would fulfill the needs. Experimental work, however, is facilitated by the use of versatile equipment. The relative ease with which the characteristics of an active network adder can be controlled led to the adoption of such a circuit.

The high gain direct coupled amplifier is well suited to the task at hand. Figure 8 illustrates the use of this amplifier as an adder (16). For general analog computation, the feedback resistor,

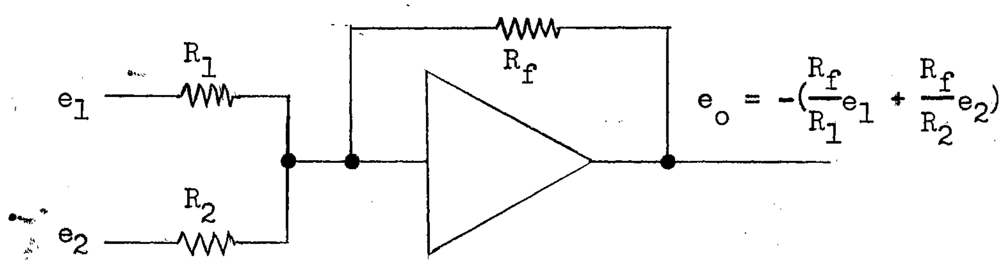

Figure 8. The High Gain Direct Coupled Amplifier As An Adder.

R_f, would be an impedance as would both R_1 and R_2. This establishes, for either input, a ratio of impedances as the amplifier transfer function. A significant feature of this arrangement lies in the inversion of the input. By this it is meant that the output is related to the input through a negative gain or more simply the output has experienced a 180 degree phase reversal.

A digression seems in order at this point. It will be seen from a discussion of β that a separate network need not be included in the circuitry to accomplish this gain.

Reference to Curve 12 will lead to the numerical evaluation of β. The plot of $1/\beta$ is indicated as a dashed, horizontal line. In terms of decibels, this line represents a 13.5 db gain. From this it may be seen that:

$$13.5 = 20\log_{10} \frac{1}{\beta} \tag{34}$$

or

$$\frac{1}{\beta} = 4.73 \tag{35}$$

so:

$$\beta = 0.211 \tag{36}$$

This value is safely within the 0.5 maximum gain requirement for stability. Interestingly enough, this very reasonable figure is obtainable by adjusting the relative sizes of the resistors in the diagram of Figure 8. In other words, the high gain direct coupled amplifier may be made to perform two functions. It is both an adder and a gain adjuster.

For practical usage, consider an R_f equal to 100,000 ohms. The voltage e_1 will, in the closed loop velocity system of Figure 7, become e_{in}. From this it follows that e_2 will be e_{fb}/β and multiplication of this quantity by β will occur in the amplifier. The gain for e_{in} should be unity. Therefore, R_1 must have the value of 100,000 ohms so that the output of the summing amplifier, due to e_{in} acting alone, will be:

$$e_o = -\frac{R_f}{R_1} e_{in} = -\frac{100,000}{100,000} e_{in} \tag{37}$$

or:

$$e_o = -e_{in}. \tag{38}$$

The gain, β, is to be included in calculating the value of R_2 so that the error signal of Figure 7 $(e_{in} - e_{fb})$ will be developed correctly by the summing amplifier. The negative sign associated with the amplifier output is at present being neglected.

From consideration of β it is evident that the ratio, R_f/R_2, must have the value 0.211. R_f has already been selected so the one unknown, R_2, may be determined.

$$R_2 = \frac{R_f}{0.211} = \frac{100,000}{0.211} \tag{39}$$

or:

$$R_2 = 474,000 \text{ ohms} \tag{40}$$

Figure 9 illustrates the input and feedback connections of the completed amplifier.

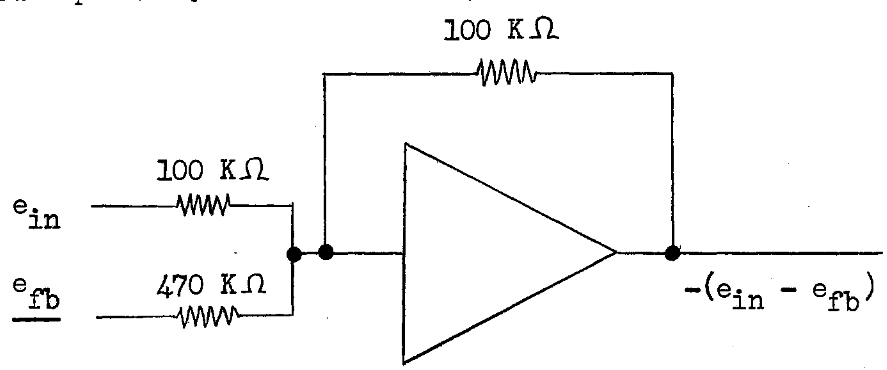

Figure 9. The Completed Summing Amplifier Circuit.

The negative sign associated with the error signal has previously been neglected. No difficulty is encountered in the final closed loop assembly, since this sign merely implies a 180 degree phase shift. Appropriate connection to the linear velocity transducer output leads nullifies this phase reversal.

The Velocity Feedback System Frequency Response

In order to prove the superiority of this system over the open loop response, a measurement of the frequency characteristics was conducted. The speaker - velocity transducer combination was again placed in free suspension. A constant amplitude, variable frequency voltage was supplied to the input terminals. The magnitude of this voltage was 0.250 volts as in the case of the open loop response in order to facilitate the comparison of the two characteristics by the direct pressure level readings (in terms of decibels) from the sound level meter. The results have been displayed as Curve 19 and the data for this curve are located in the Appendix.

The Compensated Closed Loop Velocity Circuit

The discussion of Chapter IV pointed to the development of a compensated closed system. The form of the compensating network, C(S), is shown by equations (32) and (33) while the frequency, f, is read directly from Curve 16 (f = 31 cycles per second).

If the ratio of the output, e_o, to the input voltage, e_{in}, is taken for the network of Figure 10 an expression similar to equation (32) will develop. This ratio in terms of the LaPlace operator "S" is:

$$\frac{e_o}{e_{in}} = \frac{\frac{1}{CS}}{R + \frac{1}{CS}} \qquad (41)$$

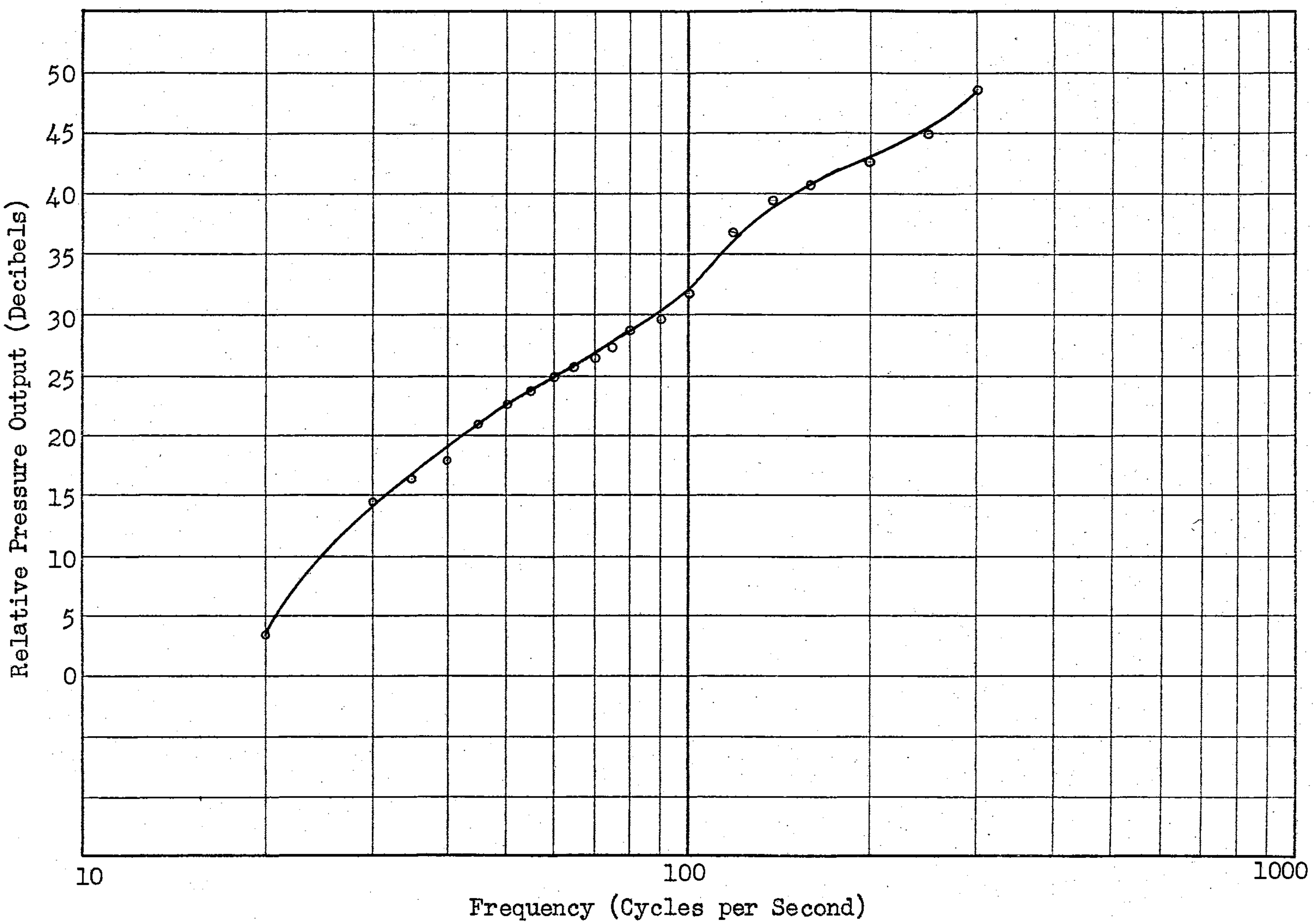

Curve 19. Frequency Characteristic of the Closed Loop Velocity System (No Compensation).

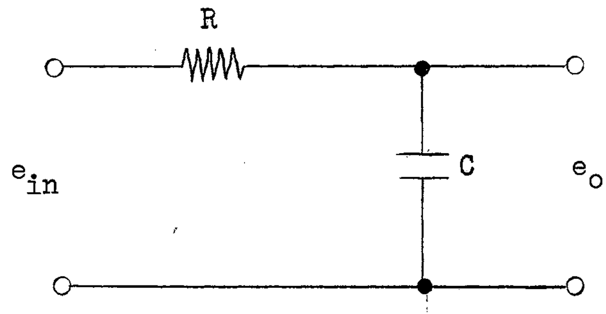

Figure 10. The Compensating Network, C(S).

or:

$$\frac{e_o}{e_{in}} = \frac{1}{RCS + 1} \,. \tag{42}$$

It is obvious from a comparison of equations (32), (33) and (42) that:

$$\tau = RC = \frac{1}{2\pi f} \,. \tag{43}$$

Now, if a value for R is arbitrarily assumed, the quantity C may be determined since f is known. This compensating network is to be inserted in the forward loop between the summing and power amplifiers. For this reason it is necessary to select an R sufficiently large to maintain only a small load on the preceding unit. An R of 100,000 ohms results in a value for C of approximately 0.05 microfarads.

Inspection of Curve 17 leads to a β of 0.355. This gain may be achieved by reducing the value of R_2, Figure 8, from 470,000 to 270,000 ohms. The final compensated system is shown in Figure 11.

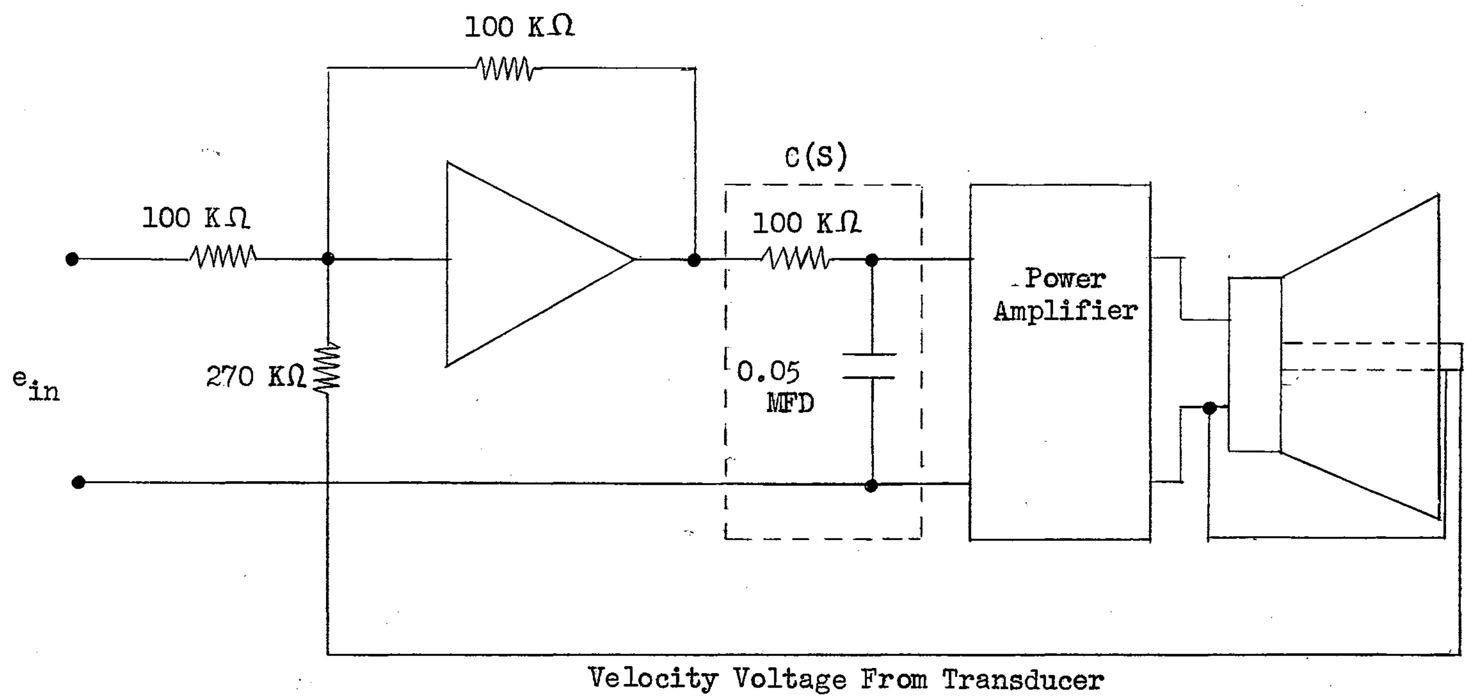

Figure 11.

The Compensated Velocity Feedback Electro-Acoustic System.

The Response of the Compensated System

Frequency response characteristics were obtained for the compensated system in the same manner as described for the previous cases. Prior to determining these characteristics, a check of the compensating network, C(S), was conducted. Curve 20 displays the data and the asymptotic approximation.

With 250 millivolts input to the overall system, the frequency was varied in discrete steps from 20 to 300 cycles per second. The acoustic pressure level (in decibels) resulting from this test is plotted against frequency on Curve 21.

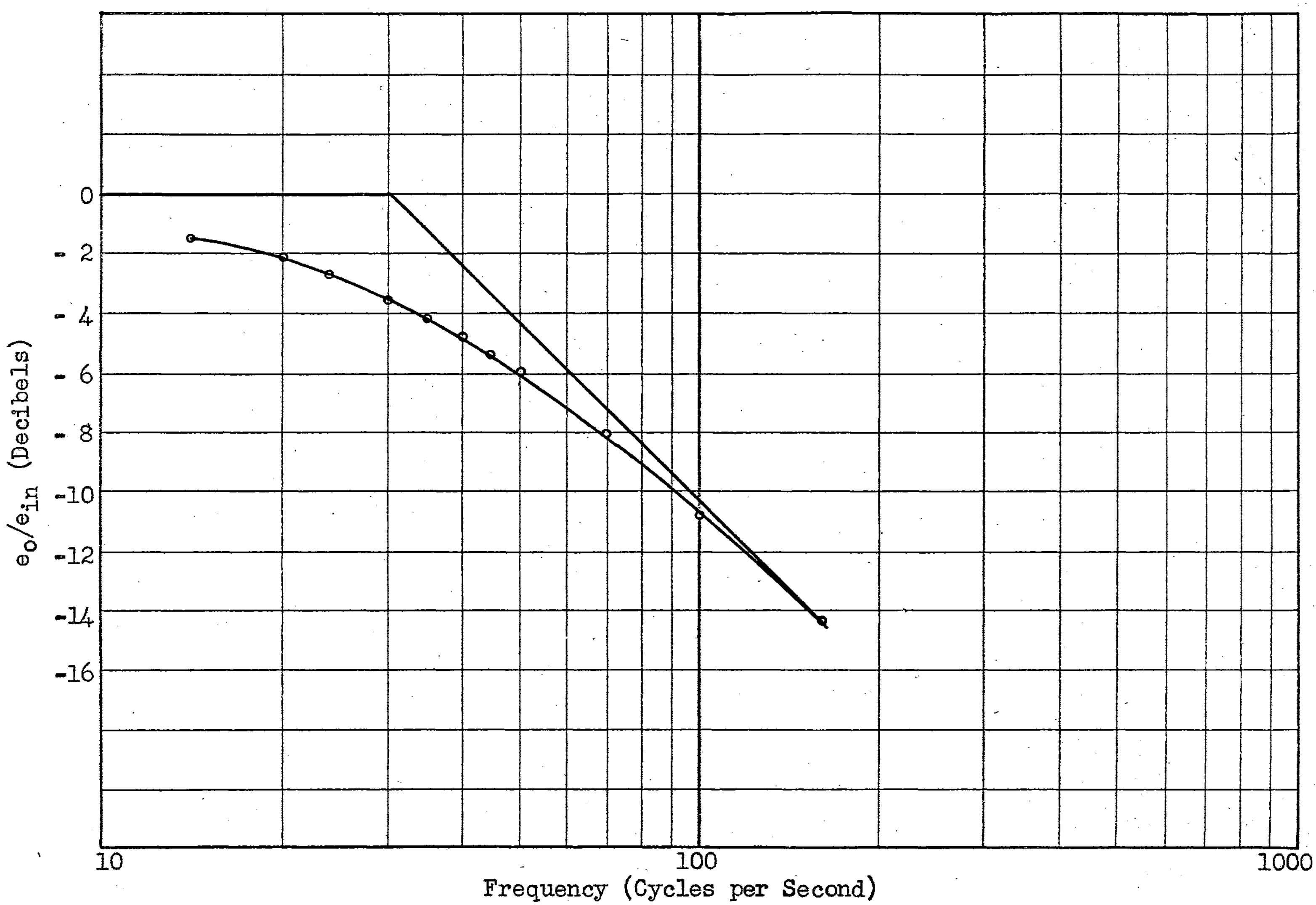

Curve 20. Response of the Compensating Network, C(S).

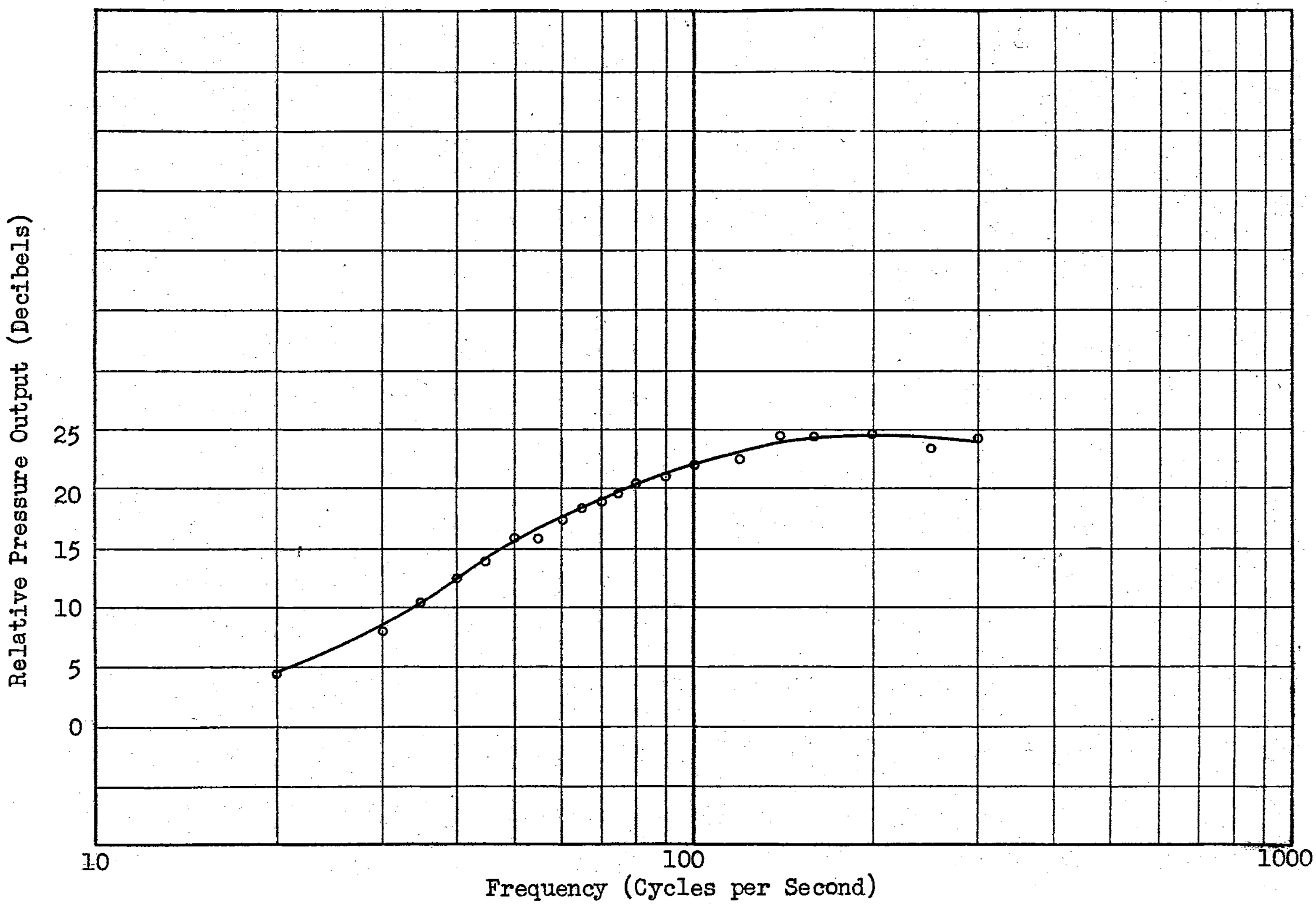

Curve 21. The Compensated System Frequency Characteristic.

PLATE V

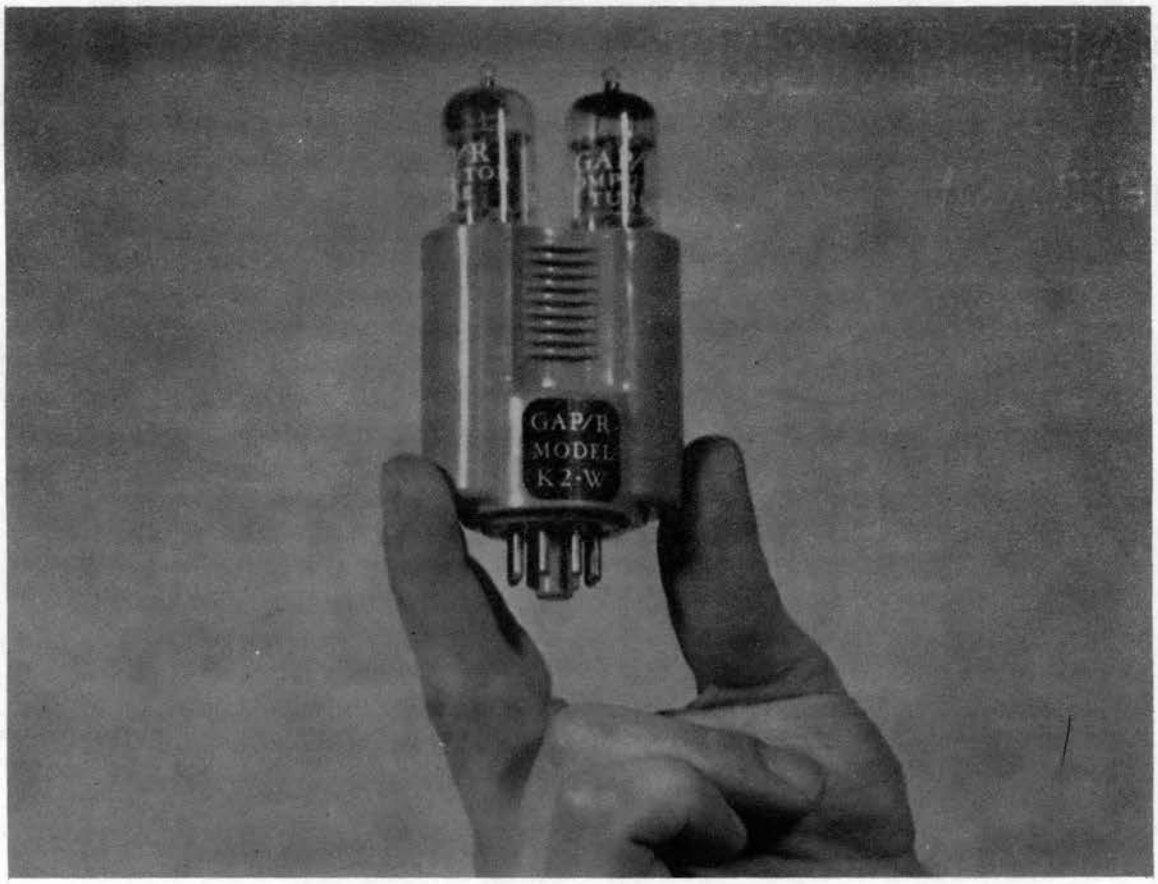

The Model K2-w Philbrick Operational Amplifier
(Gain = 15,000) Employed as a Summer and Gain Adjuster.

CHAPTER VI

RESULTS AND CONCLUSIONS

Concluding Remarks

The art of "High Fidelity" has made many startling advances in the past few years. Further progress in quality reproduction depends largely on the development of better electro-acoustic transducers and in particular, improved performance is needed in the low frequency range. Popular, present day methods of improving this low frequency response depend entirely upon open loop compensation techniques. Unfortunately the upper limit of this type of compensation seems to have been reached.

The objective of this study has been to present a different approach to the problem of low frequency compensation. This technique extends the practice of applying negative feedback around the power amplifier to encompass the amplifier-speaker combination. From the direct (velocity) feedback case the study progresses to a compensated velocity feedback circuit.

The results are very simply displayed on Curves 19 and 21. Improvement over the open loop response is evident, however, only by a comparison of these plots with Curve 5.

The most significant feature of the closed loop velocity feedback system frequency response (Curve 19) is the lack of a resonant peak anywhere below 300 cycles per second, even with a small, simple baffle board. Curve 5 displays a very marked peak. This is certainly undesirable, since it depends, not upon the input signal, but rather on the individual speaker and its environment. The elimination of the resonant phenomena does not idealize the acoustic transducer, however. A close look at Curve 19 reveals a lower output in the region below 60 cycles per second. This certainly is a disadvantage but tends to be overshadowed by the more orderly descent of the curve.

The compensated response of Curve 21 is the most satisfactory from the stand-point of response uniformity. There is no system resonance in the region of investigation and what is more, the curve is the flattest of those presented. This implies much less phase and amplitude distortion. The lack of a large output pressure level may be corrected by the application of a larger input signal. This in itself may require more equipment than in the open loop system since it suggests a higher level of preamplification.

Aside from these more obvious results there are some other improvements of great merit. An acoustic output as shown in Curve 21 requires a slow and smooth change of apex velocity, instead of the open loop characteristic of Curve 9. The equivalent electrical circuit of Figure 12 serves to illustrate the action of the speaker voice coil. R_{VC} is the voice coil resistance in ohms and L_{VC} is the inductance of this coil. The voltage source, e_M, is a representation of the voltage induced due to the motion of the coil in a magnetic field. Obviously, radical movements with changing frequency will create unusual values for e_M. If the voltage attached to terminals A and B of the speaker (Figure 12) is maintained at a constant magnitude throughout the

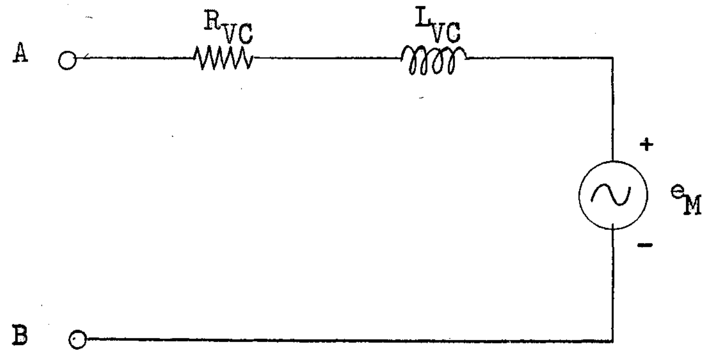

Figure 12.

Equivalent Circuit of the Speaker Voice Coil.

range of applied frequencies, then it is apparent that the current, and therefore the impedance, will vary over a wide variety of values. On the other hand, a slowly decreasing velocity voltage with increasing frequency would counteract the increase in impedance due to the reactance of the inductor. The result is a more constant load on the amplifier; hence, less distortion is generated in the output stage. This advantage alone would warrant the use of a feedback arrangement around the entire speaker-amplifier system.

One other item of interest is the high frequency response of this electro-acoustic system. If this combination is to be employed as a low frequency reproducer in conjunction with other middle and high range speakers it is desirable that the output be essentially zero for frequencies above the crossover point. The compensating network, C(S), tends to reduce the output for higher frequencies. If this circuit were used with a conventional crossover network the rate of high frequency attenuation could be greatly increased.

Recomendations for Further Study

There still remains much to be done in the area of closed loop design. The velocity transducer configuration of this study is far from a satisfactory one. Less mass and friction are desirable. As a matter of fact, the inclusion of this transducer in the voice coil space would be ideal. Mutual inductance between the voice coil and the velocity transducer would have to be held to a minimum, however. In addition, an investigation of apex position, rather than velocity, as the feedback quantity would be very worthwhile. Further development of feedback compensation might consist of closer asymptotic approximations to the real, measured curves. The use of multiple loop feedback also appears to have several advantages. With these items in mind, and the fact that speaker performance may be improved through the use of feedback, an excellent reproducing system can be developed.

BIBLIOGRAPHY

1. Read, Oliver., The Recording and Reproduction of Sound. Indianapolis, Indiana, Howard W. Sams and Co., Inc., 1952. pp. 496-518.

2. Gray, Truman S., Applied Electronics. New York, John Wiley and Sons, Inc., 1954. pp. 571-600.

3. Ryder, John D., Engineering Electronics. New York, McGraw-Hill Book Company, Inc., 1957. pp. 184-203.

4. Newitt, John H., High Fidelity Techniques. New York, Rinehart and Company, Inc., 1953. pp. 59-86.

5. Newitt, John H., High Fidelity Techniques. New York, Rinehart and Company, Inc., 1953. pp. 90-152.

6. Crowhurst, Norman H., "Feedback From the Voice Coil, Radio-Electronics, October, 1956. pp. 46-50.

7. Olson, Harry F. and Massa, Frank, Applied Acoustics. Philadelphia, P. Blakiston's Son and Co., Inc., 1934. pp. 156-217.

8. Robinson, T. Peyton, "Effects of Acoustic Proximity on Multiply Connected, Small Cone Loudspeaker." Unpublished Master's Thesis, Oklahoma State University, Stillwater, Oklahoma, 1953.

9. Olson, Harry F. and Massa, Frank, op. cit.

10. Chestnut, Harold and Mayer, Robert W., Servomechanisms and Regulating System Design. Vol. I. New York, John Wiley and Sons, Inc., 1951. pp. 297-316.

11. Truxal, John G., Control Engineers' Handbook. New York, McGraw-Hill Book Company, Inc., 1958. pp. (2-23) - (2-56).

12. Guillemin, Ernst A., Introductory Circuit Theory. New York, John Wiley and Sons, Inc., 1953. pp. 289-309.

13. VanValkenburg, M. E., Network Analysis. Englewood Cliffs, N. J., Prentice-Hall, Inc., 1955. pp. 255-260.

14. Olson, Harry F. and Massa, Frank, op. cit. pp. 245-283.

15. Chestnut, Harold and Mayer, Robert W., op. cit. p. 119.

16. Johnson, Clarence L., Analog Computer Techniques. New York, McGraw-Hill Book Co., Inc., 1956. pp. 45-63.

APPENDIX

TABLE II

OPEN LOOP RESPONSE DATA

Frequency (CPS)	Relative Pressure Output (Decibels)	Frequency (CPS)	Relative Pressure Output (Decibels)
20	67.0	80	85.0
25	69.5	90	85.5
30	73.3	100	86.0
40	79.2	120	88.6
45	82.6	140	91.0
50	85.0	160	93.2
55	87.0	180	94.0
61	87.5	200	94.5
70	85.5	250	96.5
75	85.0	300	99.5

Background Pressure Level = 50 db

TABLE III

DECIBEL GAIN COMPUTATIONS FOR THE OPEN LOOP FREQUENCY RESPONSE

Frequency (CPS)	Output Pressure (μbars)	Decibel Gain	Frequency (CPS)	Output Pressure (μbars)	Decibel Gain
20	0.433	4.77	80	3.67	23.35
25	0.604	7.66	90	3.81	23.64
30	0.914	11.2	100	3.99	24.1
40	1.822	17.21	120	5.5	26.81
45	2.76	20.9	140	7.1	29.1
50	3.56	23.06	160	8.91	31.01
55	4.34	24.78	180	10.01	32.0
61	4.75	25.55	200	10.7	32.6
70	3.81	23.64	250	13.21	34.48
75	3.67	23.35	300	18.69	37.45

Input Voltage = 250 millivolts

TABLE IV

OPEN LOOP RESPONSE OF HEATH KIT
12 INCH REPLACEMENT SPEAKER

Frequency (CPS)	Relative Pressure Output (Decibels)	Frequency (CPS)	Relative Pressure Output (Decibels)
20	59.0	100	77.0
25	65.5	120	78.0
30	69.0	140	81.5
40	73.0	160	84.0
44	77.0	180	85.0
50	80.0	200	86.0
61	79.5	250	86.5
70	78.5	300	88.0
80	77.0		
90	78.0		

Background Pressure Level = 50 db.

TABLE V

VELOCITY CHARACTERISTICS

Frequency (CPS)	Relative Pressure Output (Decibels)	Velocity Transducer Output (Volts)	Frequency (CPS)	Relative Pressure Output (Decibels)	Velocity Transducer Output (Volts)
20	64.5	0.52	80	80.5	1.05
25	66.5	0.64	90	81.4	0.85
30	71.2	0.81	100	81.8	0.75
40	76.0	1.15	120	84.7	0.645
45	78.5	1.35	140	87.5	0.465
50	82.5	1.56	160	89.5	0.42
55	83.6	1.72	180	90.5	0.38
61	80.3	1.45	200	91.0	0.345
70	80.5	1.20	250	93.5	0.27
75	80.3	1.19	300	96.4	0.245

Velocity Transducer Output = 102 millivolts per inch per second.
Input = 250 millivolts.
Background Pressure Level = 50 db.

TABLE VI

VELOCITY GAIN COMPUTATIONS

Frequency (CPS)	Velocity Transducer Output (Volts)	Velocity Gain (Decibels)	Frequency (CPS)	Velocity Transducer Output (Volts)	Velocity Gain (Decibels)
20	0.52	6.35	80	1.05	12.47
25	0.64	8.16	90	0.85	10.61
30	0.81	10.2	100	0.75	9.54
40	1.15	13.22	120	0.645	8.21
45	1.35	14.62	140	0.465	5.39
50	1.56	15.9	160	0.42	4.5
55	1.72	16.75	180	0.38	3.63
61	1.45	15.75	200	0.345	2.794
70	1.20	13.61	250	0.27	0.669
75	1.19	13.55			

TABLE VII

VELOCITY FEEDBACK ACOUSTIC CHARACTERISTICS

Frequency (CPS)	Relative Pressure Output (Decibels)	Frequency (CPS)	Relative Pressure Output (Decibels)
20	53.5	80	78.8
30	64.5	90	79.8
35	66.5	100	82.0
40	68.0	120	86.9
45	71.0	140	89.6
50	72.5	160	91.0
55	73.5	200	92.7
61	75.2	250	95.0
65	75.5	300	98.5
70	76.2		
75	77.4		

Background Pressure Level = 50 db.
Input = 250 Millivolts.

TABLE VIII

RESPONSE OF THE NETWORK C(S)

Frequency (CPS)	Output (Volts)	Gain (Decibels)
14	8.4	-1.51
20	7.8	-2.2
24	7.4	-2.64
30	6.8	-3.34
35	6.3	-4.02
40	5.85	-4.66
45	5.4	-5.35
50	5.1	-5.84
70	4.0	-7.95
90	3.2	-9.86
160	1.95	-14.2
300	1.1	-17.7

TABLE IX

THE COMPENSATED CLOSED LOOP RESPONSE

Frequency (CPS)	Relative Pressure Output (Decibels)	Frequency (CPS)	Relative Pressure Output (Decibels)
20	54.5	75	69.8
30	58.0	80	70.9
35	60.5	90	71.1
40	62.2	100	71.4
45	64.0	120	72.9
50	66.0	140	74.9
55	66.0	160	74.5
61	67.4	200	74.3
65	68.5	250	73.2
70	69.0	300	74.0

Background Pressure Level = 50 db.
Input = 250 millivolts.

VITA

Buck Ferguson Brown

Candidate for the Degree of

Master of Science

Thesis: Automatic Compensation of an Electro-Acoustic System

Major Field: Electrical Engineering

Biographical:

Personal Data: Born at Monroe, Louisiana, October 22, 1932, the son of O. W. and Roberta Brown.

Education: Attended grade and high schools in Monroe and Baton Rouge, Louisiana; graduated from Webb School, Bell Buckle, Tennessee in June, 1951; received the Bachelor of Science Degree with a major in Electrical Engineering from the Massachusetts Institute of Technology in June, 1955. The requirements for the Master of Science degree were completed in May, 1959.

Professional Experience: Employed by Convair Division of General Dynamics Corporation in Ft. Worth, Texas as an Aerophysics Engineer from April, 1955 to September, 1956 and again from June, 1957 to September, 1957. Duties consisted of preliminary design and test of the B-58 automatic control system.

Employed by the School of Electrical Engineering of Oklahoma State University, Stillwater, Oklahoma from September, 1956 to May, 1957 and employed again in September, 1957. Duties consist of teaching and research. Research is being conducted on the time series synthesis of delay type devices.